Thesis Report

Hydrodynamic Forces on a Large-Diameter Monopile during Vertical Installation

by

Lara Notenboom

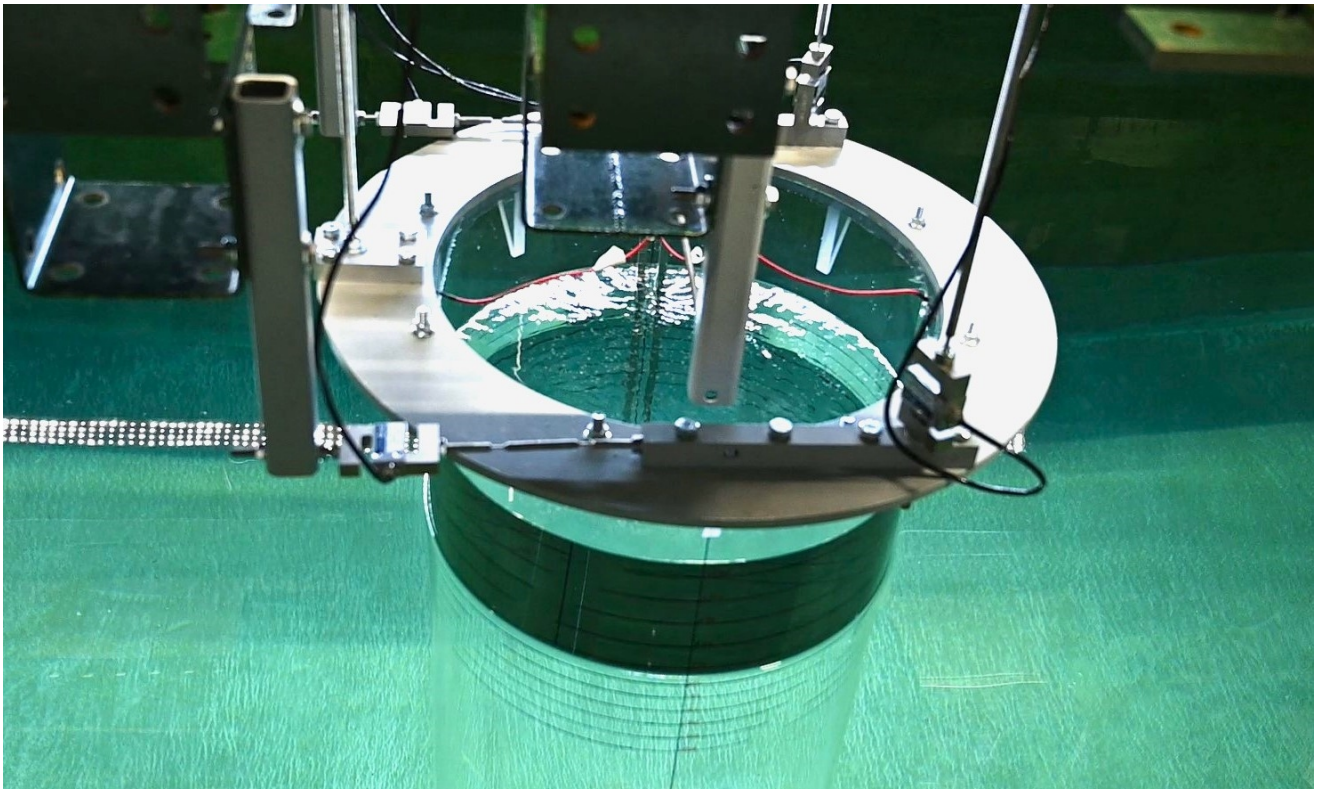

Student number: 4667433
Project duration: March 4, 2024 – February 11, 2025
Thesis committee: Dr. Ir. A. (Anna) D. Boon, TU Delft, supervisor
Dr. Ir. P. (Peter) R. Wellens, TU Delft, supervisor

TU Delft

Summary

As the shift towards renewable energy continues, larger monopiles are being installed to accommodate for the increasing size of wind turbines. To allow for safe and economical installation of these monopiles, reliable and efficient models to predict hydrodynamic forces during installation are needed. This thesis investigates the hydrodynamic forces and inner water surface behavior acting on a very large (15 meter) diameter monopile during a vertical lowering operation.

Current models, such as the Morison equation for solid cylinders in current and waves, are limited in capturing complex resonance effects of the water inside the monopile, including sloshing and piston oscillations, that could important for larger diameters. To be able to predict resonance effects of the inner water column in vertical monopiles, theory on hydrodynamic behavior of the water in moonpools might be a solution. However, this theory is limited to enclosed water volumes surrounded by the ship's volume, which is different from a thin-walled cylinder like the monopile. The objective of this study is to address the gaps in the research on solid cylinder and moonpools and use the existing theory to improve predictions on vertical monopiles through experimental and theoretical analysis.

The research involves experimental wave tank tests using a scaled monopile model at different drafts, subjected to monochromatic waves of varying length and height. . Measurements included forces, moments, and inner water column dynamics, at three distinct drafts, to study resonance effects. To find the relevant hydrodynamic forces, the measurements were analyzed using both time-domain and frequency-domain methods. The results of the monopile experiments are compared to existing theoretical prediction methods for solid cylinders and moonpools.

The Morison equation was found to be a reasonable estimate for hydrodynamic forces, even though it was originally developed for solid cylinders. Morison's equation was found to be applicable to vertical hollow cylinders for most waves, except for shorter wavelengths. Notably, for the shortest draft, the Morison equation remained a good estimate even for wavelengths 6 times larger than the model length, despite theoretical guidelines suggesting applicability only from 10 times the wavelength. As monopile diameters increase, the Morison equation will be less applicable for the prediction of forces and moments in a realistic offshore scenario for the North Sea. This means other methods, like finite element analyses, have to be used to be able to get a good estimate of wave forces and moments on a large-diameter monopile.

Resonance phenomena, including sloshing and piston oscillations, were observed at both shallow- and deeper drafts, with frequencies aligning with predictions based on moonpool theory. Comparing the moonpool prediction for the height of the water level to the measured water level results in a conservative estimate by the moonpool theory of 30% to 300% larger amplitudes than measured for the monopile. This discrepancy cannot be explained by the viscous effects during resonance, because the discrepancies between moonpool theory and measured in the monopile were lowest when resonance modes were induced in the monopile. Therefore, further research into these phenomena is recommended.

Despite the presence of these resonance modes, no significant differences in the resulting forces were observed, indicating that resonance effects have limited impact on the hydrodynamic forces experienced by the monopile during vertical lowering operations. The conclusion can be drawn that the impact of these modes on the vertical lowering operation of a large-diameter monopile is limited, especially in an offshore installation, where the monopile is supported in all directions and can be shielded by the installation vessel.

Future research could explore alternative methods for more accurately predicting hydrodynamic forces on large-diameter monopiles, especially in sea states where shorter waves are present, to refine predictions and improve operational safety.

Preface

Starting off, I would like to thank my thesis supervisors Dr. Ir. Anna D. Boon and Dr. Ir. Peter R. Wellens for their guidance and expertise, but more than that I am very grateful for your encouragement and belief in me throughout this project. I would also like to thank Dr. Ing. Sebastian Schreier and Ing. C. Peter Poot for their assistance during the experiments, as well as all the other staff at the Ship Hydromechanics Lab who offered their help along the way.

A special thank you to my friends and family for being there. Whether it was through motivation, distractions, or just keeping me going. I couldn't have done it without you.

Lara Notenboom
Delft, February 2025

Contents

1 Introduction

This chapter introduces the background and motivation behind the study, focusing on the challenges in hydrodynamic predictions for large diameter monopiles during lowering operations. The scope of the research is presented along with the key research questions, laying the foundation for the scientific investigation into monopile behavior in wave conditions.

1.1. Problem definition

In recent years, wind energy plays an increasingly significant role in meeting growing energy demands. Offshore wind energy offers vast potential for generating clean electricity, since wind offshore is generally stronger and more consistent. As a result, there has been a substantial increase in the installation of wind turbines offshore. Monopiles have become the most dominant foundation for offshore wind turbines due to their cost-effectiveness and reliability. However, offshore wind turbine generators continue to evolve in terms of power capacity and size, as accessible shallow-water sites have already been exhausted in some parts of the world, and around 80 percent of global offshore wind resources are in water over 60m [1]. Consequently, the demand for larger monopiles has increased.

One of the problems the industry is facing in the demand for larger monopiles, is related to the installation of the monopiles offshore. Larger diameter monopiles might show different hydrodynamic behavior than the monopiles currently used. This is not only due to the increase in size, but the increase in free-surface area inside the hollow monopile seems to become more important for the hydrodynamic behavior, as the water inside the monopile could have resonant modes in other frequency regions than we are used to for current monopiles. It is very important to investigate the effects of the increasing diameters, because installing monopiles offshore is a very risky procedure and accurate prediction of hydrodynamic behavior in certain sea states is required for safety reasons. Additionally, accurate prediction of the behavior could result in an increase of the weather window in which monopiles can safely be installed, so weather downtime can be limited, which is naturally desirable from a financial objective [2].

1.2. Objective of the thesis

The goal of the project is to provide a comprehensive analysis of a specific stage within the installation process of a monopile, namely the lowering of the vertical monopile through the water column. This analysis will be focused on large diameter monopiles and their resonance modes, specifically the sloshing- and piston mode resonance. Changes in hydrodynamic behavior at different drafts are expected, therefore different drafts will be included in the analysis.

1.3. Research Questions

The main research question for this study is:

What are the hydrodynamic forces acting on a large diameter monopile during a vertical lowering operation?

The aim is to answer this question using the following sub questions:

- What wave and current conditions are important to analyze for this procedure?
- What are the differences in hydrodynamic forces between a solid cylinder and a monopile?
- What are the differences in hydrodynamic forces between a moonpool and a monopile?
- Which resonant modes of the water inside the monopile can we expect to be important in a monopile lowering operation?
- How does the draft influence the hydrodynamic forces for a monopile?

1.4. Research methods

Firstly, a literature research will be conducted to gain knowledge about the subject, provide insight and define the research gap. The literature research will focus on the knowledge that is already available about cylinders in waves and current, zooming in on the hydrodynamic behavior of cylinders with a free end and hydrodynamic behavior of fluid in gap, such as a moonpool. Furthermore, it will have a look into the studies already conducted on monopile installations offshore.

Using the knowledge on cylinders and moonpools, we will analytically determine the expected hydrodynamic behavior of the combination of the two, i.e. monopiles. To validate the predictions, experiments will be conducted.

Experiments are performed in a wave tank, using a scaled monopile model subjected to monochromatic waves. Measurements include wave-induced forces, moments, and inner water column behavior. The setup accommodates varying drafts to assess their effects on hydrodynamics.

Data analysis combines time-domain and frequency-domain methods to identify trends and resonance phenomena. Experimental results are compared to theoretical predictions, highlighting discrepancies and providing insights into the limitations of existing models.

2

Literature and Theory

This chapter reviews the relevant scientific literature on hydrodynamics of cylinders and moonpools, focusing on the differences in fluid dynamics for solid cylinders, monopiles, and moonpools. The main theories and experimental findings from existing studies are summarized to highlight the gaps this research aims to address.

2.1. Introduction of Background and Research Gap

Large-diameter monopiles are essential components in offshore wind turbine installations, providing stable foundations in challenging marine environments. However, as monopile diameters increase, their hydrodynamic behavior changes, introducing new challenges in accurately predicting forces during installation. While existing theories for solid vertical cylinders and moonpools offer valuable insights, they fail to fully describe the behavior of monopiles, particularly the correlation between hydrodynamic forces and internal water column dynamics.

This thesis focuses on the inertia-dominated nature of the monopile's hydrodynamic behavior, driven by its low Keulegan-Carpenter (KC) number and the dominance of inertial forces over viscous effects. Although viscous effects around the sharp edges and the submerged free end of the monopile present interesting problems, the primary focus is placed on understanding inertial forces and the movement of the inner water surface. This decision reflects the monopile's unique characteristics, the resonance modes of the inner water column, and the practical importance of these effects during offshore installation.

This chapter explores how hydrodynamic forces on monopiles can be understood through existing theories for solid cylinders and moonpools, identifying their limitations and highlighting the need for alternative approaches. In section 2.2, the Morison equation, widely applied to solid cylinders, is introduced first. Its limitations for short-wave conditions, where diffraction effects become significant, are discussed, leading to the inclusion of diffraction theory and computational tools like ComFLOW. Next, in section 2.3 moonpool theory is reviewed to assess its applicability to monopile dynamics, particularly in describing resonance phenomena.

The reasoning behind prioritizing inertial forces and inner water surface dynamics over viscous effects is addressed in section 2.2.4. This chapter ultimately describes the analytical and experimental methodologies used in this thesis to bridge the theoretical gaps and improve the understanding of monopile hydrodynamics.

2.2. Hydrodynamics of Solid Cylinders

This section will provide theory on solid vertical cylinders. To gain a better understanding of the hydrodynamic behavior of a monopile that is lowered vertically into in the water, we can make use of the already widely available research that has been done on cylinders in current and waves [3], [4], [5], [6]. The difference with a monopile is that most research on cylinders is for solid, instead of hollow, cylinders. However, the available literature provides a good overview of the hydrodynamic behavior of the exterior of the monopile, without looking too much into the behavior of interior part yet.

During the installation of a monopile, there are some differences with the flow theory for vertical cylinders without presence of an air-water interface. The first being that the cylinder or monopile is surface-piercing and thus the existence of a air-water interface needs to be taken into account. Another difference is that when the monopile is lowered into the water, it will have a lower free end. This will have influence on the flow structures around that part of the cylinder.

2.2.1. Overview of the Morison Approach

The estimation of hydrodynamic forces on monopiles relies on analytical models developed for various cylindrical structures. For monopiles, a commonly used model is the Morison equation, originally formulated for solid cylinders [4]. This equation accounts for both inertia and drag forces through the inertia (Cm) and drag (Cd) coefficients. At the base of this equation lie some assumptions. The first is assuming small amplitude waves, so linear wave theory (Airy wave theory) can be applied. The second is assuming monochromatic waves with wave height H, wave period T, and water depth h. The final assumption is that the water inside the hollow cylinder is similar to a solid cylinder with diameter D in terms of inertia.

The wave force on a vertical cylinder can be calculated using the Morison equation, which is suitable for structures where both inertia and drag forces are significant. The Morison equation is given by equation 2.1

$$F(t) = F_D(t) + F_I(t) \tag{2.1}$$

where: $F(t)$ is the total wave force, $F_D(t)$ is the drag force and $F_I(t)$ is the inertia force.

The drag force per unit length of the cylinder is given by equation 2.2

$$F_D(t) = \frac{1}{2}\rho C_D D|u(t)|u(t) \tag{2.2}$$

where: ρ is the water density, C_D is the drag coefficient, D is the diameter of the cylinder and $u(t)$ is the water particle velocity.

The inertia force per unit length of the cylinder is given by equation 2.3

$$F_I(t) = \rho C_M A \frac{du(t)}{dt} \tag{2.3}$$

where:

- C_M is the inertia coefficient
- A is the cross-sectional area

Using linear wave theory, the horizontal water particle velocity $u(t)$ at the surface (z = 0) is given by equation 2.4.

$$u(t) = \frac{H}{2} * \omega \frac{cosh(k(h+z))}{sinh(kh} \cos(\omega t) \tag{2.4}$$

and the horizontal water particle acceleration $\frac{du(t)}{dt}$ by equation 2.5

$$\frac{du(t)}{dt} = -\frac{H}{2} * \omega^2 \frac{cosh(k(h+z))}{sinh(kh} \sin(\omega t) \tag{2.5}$$

To calculate the total wave force over the height of the cylinder H_c, integrate the drag and inertia forces from the water surface to the bottom of the cylinder, the draft through equations 2.6 and 2.7.

$$F_D(t) = \int_0^{draft} \frac{1}{2}\rho C_D D|u(t)|u(t)\, dz \tag{2.6}$$

$$F_I(t) = \int_0^{draft} \rho C_M D \frac{du(t)}{dt}\, dz \tag{2.7}$$

Combine the drag and inertia forces to get the total wave force in equation 2.8.

$$F(t) \approx \frac{1}{2}\rho C_D D H_c \left(\frac{\pi H}{T}\right)^2 \cos^2\left(\frac{2\pi t}{T}\right) + \rho C_M D H_c \left(-\frac{2\pi^2 H}{T^2}\right) \sin\left(\frac{2\pi t}{T}\right) \tag{2.8}$$

In practice, the values of Cm and Cd are generally based on experimental or computational studies of solid cylinders. Applying this equation to hollow monopiles, that are surface piercing and have a free submerged end, requires adjustments to these coefficients to capture the influence of the inner water column, the surface effects and the free-end effects. This section presents the Morison equation and discusses the adjustments that need to be made to make the equation suitable for a hollow-, surface-piercing cylinder. First, the determination of the coefficients for solid cylinders is explained.

The inertia coefficient Cm has a theoretical value of 2 in a potential flow. Where 1 is made up of the ambient pressure field and 1 is from the flow disturbance caused by the cylinder. In practice the contribution from the ambient pressure field having a value of 1 is considered to be acceptable. The coefficient from the flow disturbance is much less certain, because the vortices in the wake, in a real flow, disturb the theoretical flow pattern used to determine the value of this coefficient. Many researchers have conducted laboratory tests determine Cd and Cm coefficients for all kinds of situations. The results of Sarpkaya's experiments with smooth cylinders in U-tubes are presented as graphs of the coefficients Cd and Cm as functions of Sarpkaya beta and KC number [3].

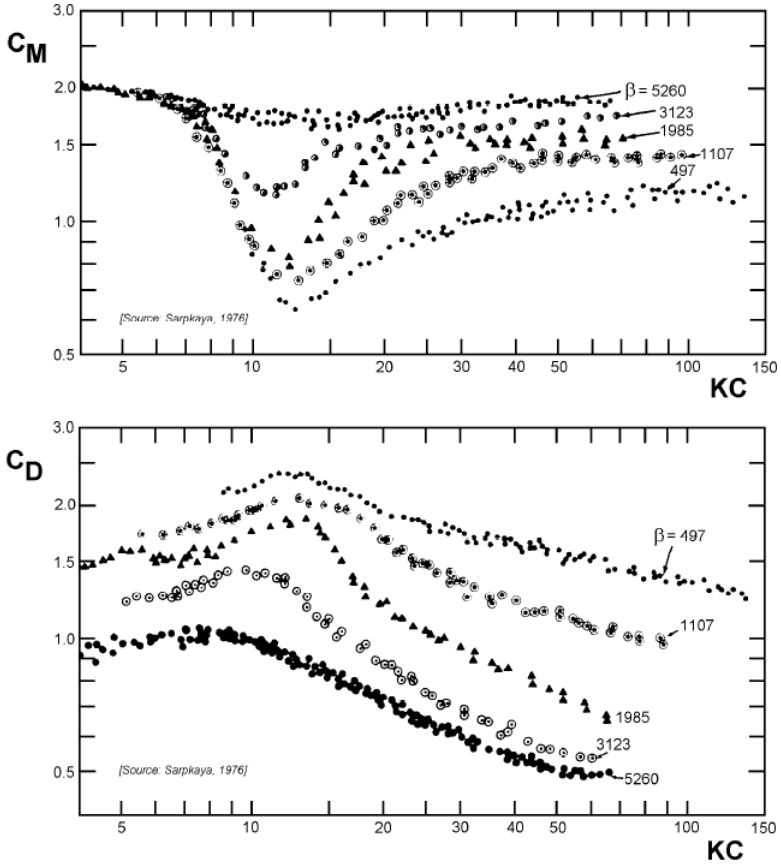

Figure 2.1: Laboratory measurement result from Sarpkaya [3]

For deep water, the KC number can be computed using equation 2.9.

$$KC = 2 * pi\frac{\zeta_a}{D} \tag{2.9}$$

In this project, the KC number have very low values of 0.76 at maximum. Also, the monopile model has a very smooth surface. From this information it could be concluded that Cm in this case has a value of 2.0 and Cd a value of 1.0. However, this problem is different from the solid cylinders that were experimentally tested and from which the coefficients for the Morison equation have been determined. Starting with the fact that in this problem, the cylinder is piercing the water surface. A surface piercing cylinder can radiate and diffract waves in a more complex manner than a fully submerged cylinder. These effects can change the added mass and drag behavior, especially near the water surface where wave interaction is more significant. The differences in this problem compared to most available research are:

- **The cylinder is surface-piercing**: near the water surface, nonlinear effects due to wave breaking, sloshing, or free surface deformation can significantly impact the forces acting on the cylinder. These effects are generally not captured by linear wave theory, which assumes small wave amplitudes and a calm free surface. In reality, wave nonlinearity near the surface-piercing cylinder could change the velocity field or cause additional forces, even if small.
- **The cylinder is hollow**: the cylinder being hollow instead of solid may reduce the overall inertia or added mass and lead to different flow behavior inside and outside the cylinder. In a hollow cylinder, a water column is present inside the cylinder potentially causing additional resonance modes and water movement to happen that are not accounted for in the standard Morison formula. The hollow part could also reduce the drag, especially if water can flow through the interior or around the submerged ends more freely.
- **The cylinder has a free submerged end**: a free submerged end can cause differences in how the flow behaves around the cylinder. At the free end, vortex shedding and flow separation could occur differently compared to a fully submerged body, contributing to drag more than using simple drag terms.

These differences are important to consider when using the Morison approach for this problem. Previous research shows that the Cm and Cd coefficients in the equation can be modified to capture the effects of such problems [5]. It shows that the Cd value slightly decreases to 0.8 for cylinders that are surface-piercing and have a free submerged end. However, changing Cd has negligible influence on the output of the Morison equation for this data, since the problem is inertia dominated and the contribution of drag force is small.

For Cm however, the value is hard to determine and validation data from previous research for this specific problem is limited. In fast current and low waves, free surface effects are found to increase Cm [7]. However, wavy flow for very low KC numbers, as in this experiment, shows very low values for Cm in some cases below 0.2 for sharp edged rectangular solid cylinders that are surface piercing and have a submerged free end [6].

In the case of a monopile that is lowered through water, free surface effects will be present. The flow at the free surface is known to show different complex structures in the vicinity of the cylinder; a bow wave appears at the front, which then spills over the cylinder to generate the near wake. The bow wave itself can break up and develop into a fountain at higher flow velocities. Yu et al. studied free surface effects on a cylinder in 2008 [8], and found that the free surface delays the vortex generation in the near wake, leading to reduced vorticity and vortex shedding. However, this study also showed that for higher Reynolds numbers, a negative pressure zone could develop in both the air and water regions near the free surface leading to a significant increase of drag force on the cylinder in the vicinity of the free surface. Yet the study shows that at very high Reynolds numbers above 1.0E5, 2D vortex structures prevail in the wake and the flow behaves like a 2D flow without a free surface.

Journée and Massie [3] stated that the dimensionless Froude number is primarily associated with free surfaces effects, expressed in equation 2.10. In this expression u_a is the local flow velocity in m/s, g is the acceleration of gravity in m/s^2 and D is the diameter of the cylinder.

$$F_n = \frac{u_a}{\sqrt{gD}} \tag{2.10}$$

Yu et al. [8] already mentioned that the free surface's delaying effect on the vortex generation in the near wake is more pronounced at higher Froude numbers and that the mean drag force shows a small decrease with higher Froude numbers. This is supported by Koo et al. in 2014 [9] that stated that different Froude numbers as well as increasing Reynolds numbers from subcritical to critical, result in significant changes in flow features near the free surface. For the case of monopiles lowered down in water, low Froude numbers are expected as the characteristic length of a monopile, thus the diameter, is relatively small and the flow velocity in the North sea is not high enough to consider Froude numbers leaning towards critical flow regime, which happens for Fr = 1.0.

Depending on the flow conditions at the monopile installation site, the free surface may or may not have a large effect on the pressures and forces the monopile experiences. It is important to consider the region of Reynolds and Froude numbers at the monopile installation site, as hydrodynamic behavior can differ.

Another distinction that the procedure of lowering a monopile through water has opposed to the Morison flow theory is that the monopile has a free lower end. Benitz et al. did experimental measurements of flow past free surface piercing, finite length cylinders in 2016 [5]. This study simulated varying aspect ratios, the ratio of submerged length (or draft) of the cylinder over the diameter of the cylinder. They did this by varying the draft of the cylinder and keeping a constant diameter. This is very interesting for a study into the hydrodynamic behavior of the process of lowering a monopile through water, because in this process different drafts will have to be investigated. They found that the presence of a free-surface and a truncated cylinder end affects the structural loading, in both magnitude and frequency. These alterations to the loading behavior are dependent on the aspect ratio, such that at small depths of penetration, the drag is greatly diminished and the periodicity of loads from vortex shedding is absent.

At higher aspect ratios the drag coefficient was found to be nearly constant. A sharp drop in the drag coefficient was observed at an aspect ratio equal to 2, as the flow can travel under as well as around the cylinder. Tip vortices were seen to dominate at small aspect ratios, while more pronounced vortex sheets were observed behind cylinders with larger aspect ratios.

For the lowering process of a monopile this has interesting consequences as it means that different drafts have different effects on the dominating loading behavior and it can give important insights to know for which drafts a certain loading behavior is dominant.

Additionally, studies of Mohseni et al. in 2018 [10] and Chen et al. in 2022 [11] observed various turbulent structures for a surface piercing cylinder with a free end such as wave-induced vortices below the free surface and tip vortices near the free end. These studies were conducted at higher Froude numbers than we expect for the lowering of a monopile in water so comparing these outcomes to the monopile might not be a good comparison. However, it is interesting to see the fluid behavior around the free end in these studies, and for the monopile we still need to take into account that it is a hollow structure instead of the solid ones studied here. The difference is that the fluid does not only encounter a free end, but also sharp edges of the thin-walled monopile, which is usually a cause for vorticity.

Taking into account all these differences, it could be possible to adapt the Morison equation for this problem with modified Cm and Cd coefficients. However, there are other limitations to the Morison approach. These will be discussed in the next section.

2.2.2. Limitations of Morison Approach for Present Problem

For the Morison equation to accurately predict hydrodynamic forces, a high wavelength-to-diameter is required, with wave lengths ideally being 10 to 20 times the monopile diameter [3]. This limitation implies that force predictions using the Morison equation will become less accurate as the wavelength decreases, which is expected to affect force the comparison to the measurements for smaller waves in this study. The limitation of the Morison method to waves with a wavelength 10 to 20 times longer than the diameter of the vertical cylinder can be explained by examining the fundamental assumptions

underlying this approach. The Morison equation was originally developed to calculate hydrodynamic forces on a structure subjected to a steady current [4]. When applied to wave conditions, the water particle velocity associated with the wave motion is treated in a similar manner to a current. This assumption holds well for long waves relative to the object's size, as the wave-induced particle velocities behave much like the steady flow of a current over the object. However, for shorter waves, this assumption breaks down. The water particle velocity varies significantly over a short duration as the wave passes the object, unlike the consistent flow of a current. As a result, the Morison method fails to accurately capture the hydrodynamic forces for shorter wavelengths, leading to discrepancies between analytical predictions and measured results.

It is established now that the Morison equation has not shown to accurately predict forces for short waves as in this problem. In the next section another way of predicting the forces more accurately using diffraction theory is described.

2.2.3. Diffraction Theory

For shorter wavelengths or scenarios where wave diffraction becomes dominant, diffraction theory provides a more appropriate framework than the Morison equation. Diffraction theory accounts for the interaction of waves with the structure, including wave scattering and reflection, which are critical in the regime where the wavelength is comparable to the monopile diameter. In these cases, the hydrodynamic forces are primarily determined by wave pressure distribution rather than drag or inertia components alone.

Using computational fluid dynamics (CFD) simulations offers an alternative method to predict hydrodynamic forces accurately under these conditions. These methods use a volume-of-fluid approach to model free surface flows, capturing the complex interactions between waves and structures, including non-linear and viscous effects.

The advantages of using CFD are that it accounts for the hollow nature of the monopile and the effects of the inner water column. CFD can capture non-linear effects such as sloshing inside the monopile or viscous effects near the free end.

2.2.4. Prioritization of Inertial Effects

The focus on inertial effects over viscous effects in this study is driven by several factors:

First is the low Keulegan-Carpenter number. The experiments are conducted at low KC numbers (KC<3), where the flow is inertia-dominated. Under these conditions, the contribution of drag forces is minimal, making the accurate estimation of inertia forces critical for understanding the overall hydrodynamic behavior. A second reason is the importance of the resonance of the inner water column. Sloshing and piston mode resonances in the inner water column significantly influence the forces and moments acting on the monopile. These inertial phenomena are pivotal for capturing the dynamics of the system during lowering operations. Then there are also practical constraints. Scaling realistic offshore waves using the Reynolds number with the necessary geometric scaling factor results in wave conditions that the wave maker in the wave tank cannot reliably reproduce. This limitation significantly impacts the accuracy and reliability of the scaled-down experimental conditions. Finally, given the limited scope and time available, the study prioritizes phenomena that dominate the hydrodynamic response. While viscous effects, particularly at the free submerged end, are of interest, they are considered secondary in this context.

The decision to focus on inertia aligns with the objective to bridge the gap between solid cylinder and moonpool research. By addressing the challenges posed by the inner water column and free surface interactions, this study contributes to a more nuanced understanding of the hydrodynamic forces acting on monopiles during offshore installation.

2.3. Moonpool Hydrodynamics

A moonpool is a vertical opening or gap through a floating body's hull and deck, allowing water to flow through. It is used for various offshore operations such as drilling, pipe laying or diver recovery. The hydrodynamic behavior of moonpools is interesting as they interact with waves and ship motion. In regard to the monopile problem, the moonpool is interesting because the structures have in common that both feature a column of water surrounded by walls. The difference with the moonpool is that

around the inner water column, there is a substantial volume, whereas the monopile's walls are thin and in direct contact with the water on the outside.

Studies on moonpools serve as a valuable source of information when investigating the hydrodynamic behavior of large monopiles, as they offer insights into fluid behavior when the fluid is trapped by a surrounding structure. This study is focused on the hydrodynamic behavior of large-diameter monopiles when they are lowered down through the water. During this process, the monopile will be (partly) submerged and a column of water with a free surface will be present inside the monopile. For this purpose it is important to understand the behavior of fluid both inside and outside the monopile. This chapter will focus on the fluid behavior inside moonpools, to get a better understanding of fluid behavior inside monopiles.

2.3.1. Resonance Phenomena in moonpools

The water inside a moonpool is in contact with the surrounding water around the floating structure. When there are motions in the water such as waves or current, or when the floating structure around the moonpool moves, the water inside the moonpool will move as well. At certain oscillating frequencies, the water motion might show resonance which could lead to unexpected loads.

A common resonant behavior for a moonpool is the sloshing mode, where the fluid moves longitudinally or transversely back and forth inside the moonpool. It occurs due to the motion of the vessel or platform, or due to wave induced pressures causing water motion. Molin [12] was one of the first to study the hydrodynamic behaviour of moonpools. In his study in 2001 he considered rectangular moonpools and showed that the natural frequencies of the longitudinal sloshing modes increase when the draught and width of the moonpool, with constant length, decrease. Consequently, this means that when a moonpool with constant length and width, but an increasing draught over time, the natural frequency of the longitudinal sloshing modes decrease over time. During the process of lowering down a monopile in water, one will find decreasing values of natural frequencies of the longitudinal sloshing modes over time, according to this theory.

Another typical fluid motion is the piston motion, where the mean surface inside the moonpool experiences vertical oscillations. The amplitudes of the oscillations may be substantially larger than the actual ship motions. Lu et al. in 2010 [13] studied the fluid resonance in narrow gaps between structures and found piston-mode resonant behavior. The maximum resonant wave height in the gaps was up to 4 times the incident wave height. This piston-mode resonance behavior occurred at distinct frequencies. As Molin [12] stated, in the piston mode, the water inside the moonpool heaves up and down more or less like a rigid body. Because of the possibly large resonant motions, it is important to calculate the amplitude of these resonant modes and to precisely locate their frequencies with regard to the frequencies of the most energetic waves.

Many studies have been conducted on the moonpool problem. A recurring topic is the discrepancy between experimental outcomes and results calculated with potential theory [13], [14], [15], [16]. Linear, inviscid results generally seem to over-predict resonant motions of the moonpool, because viscous damping is not accounted for.

Faltinsen, Rognebakke and Timokha [14] studied piston-like motions inside the moonpool for finite water depth. Comparing linear inviscid results to experimental data, they found small discrepancies. They argued that vortex shedding at the moonpool edges may cause substantial damping of the motion and therefore contribute to the discrepancy, but vortex shedding alone cannot explain the discrepancy between theory and experiment for the experimental cases considered, because they used small forcing amplitudes and vortex-induced forces are velocity dependent. They stated that in their experiments, the free-surface nonlinearity associated with potential-flow effects might have been an important cause for the discrepancy.

Kristiansen [15] studied the discrepancy between linear theory and that observed in reality for a case with similarities to a moonpool. He stated that there are three candidates explaining the discrepancy. (1) effects due to the nonlinear free-surface conditions, (2) flow separation and (3) boundary layer effects. In his experiments, the results from simulations by a nonlinear wavetank including flow separation compared well with the experimental results, in contradiction to results from linear simulations or results from the nonlinear wavetank without flow separation. Hence, he strongly suggests that flow separation causes the majority of the discrepancy.

This suggestion is supported by research of Lu et al. in 2010 [13] and [16] where, in piston-mode problems, they observed complex vortex structures, shedding, and flow separation, explaining the overestimation of wave height in potential flow models and highlighting the importance of accurately modelling viscous damping in moonpool problems.

Following these studies, researchers became increasingly interested in the viscous effects for moonpool problems, so they explored various methods to develop a deeper understanding of the phenomena. In 2012 Kristiansen & Faltinsen [17] and in 2015 Fredriksen et al. [18] found that with a computational fluid dynamics (CFD) solver, the viscous damping could be modelled accurately and discrepancies between experiments and numerical results can be avoided this way. However, employing computational fluid dynamics (CFD) techniques can be computationally intensive.

Studies on moonpools serve as a valuable source of information when investigating the hydrodynamic behavior of large monopiles, as they offer insights into fluid behavior when surrounded by a structure. However, a significant distinction between moonpools and monopiles lies in the fact that moonpool theory typically involves a substantial volume of floating structure surrounding the moonpool, whereas the monopile is characterized by thin walls. The presence of this floating structure volume around the moonpool contributes to the displacement of a larger volume of water during heave motion. This displacement occurs not only towards the sides but also through the opening of the moonpool. Consequently, it is expected that the hydrodynamic effects in a case with a monopile will yield different outcomes compared to those observed in a moonpool scenario. Therefore, understanding of the fluid behavior outside the monopile and the complex fluid behavior around the monopiles' lower free edges is important.

Various studies show that nonlinear damping (due to flow separation, vortex shedding, free-surface effects) at the moonpool or gap entrance is dominant compared to wave radiation damping [13], [15], [17], [18], [19]. Therefore it is expected that viscous damping will also be important in the case of monopiles.

A big difference still is that moonpools have a substantial volume of floating structure surrounding the entrance. During heave motion, this results in more water displacement beneath the hull compared to that which would occur with a thin-walled monopile, which could cause different fluid behavior around the sharp edges than one would find in a moonpool. This is why the study of Ravinthrakumar et al. [16] is particularly interesting, because studying a larger moonpool to ship ratio of 1/2, they get a bit closer to the properties of the monopile problem. In this study, differences in hydrodynamic behaviour between the smaller and larger moonpools, such as swirling-type sloshing and secondary resonance (where higher harmonics in the motion of the free liquid surface cause resonant motion at natural sloshing periods other than the primary resonance periods) are mentioned. The nonlinear effects mentioned are excited in a range of wave periods where it is expected that a realistic sea environment will contain significant wave energy. This is most prominent in the largest moonpool. This might be an indication that this will get even more important in larger moonpool to hull ratios, approaching that of a monopile. Additionally, this is providing reasons to believe that there will be differences in hydrodynamic behavior between smaller diameter monopiles and larger diameter monopiles as well, as for large diameter monopiles the moonpool to ship ratio will be even larger.

Furthermore, the study of Han et al. [20] is also of major importance for the present study on monopiles, because there are few studies conducted on both three-dimensional and circular moonpools. These are two properties that are important to investigate in the study of the hydrodynamic behavior of monopiles. Han et al. [20] stated that the damping effect due to flow separation from the inlet of a three-dimensional moonpool is still an open question, yet very important for practical application in the offshore industry. Different components of the wave response in the moonpool, including the mean elevation and second harmonic, were observed in their experiment. The conjectured sources of such components (except the first harmonic) are the variation of the instantaneous position of the free surface inside the moonpool and the nonlinear quadratic damping induced by flow separation. However, they also stated that it should be noted that the KC values used in this experiment may be smaller than those in practical application, and the effect of larger KC values should be studied further.

Extensive research has now been conducted on fluid behavior around vertical solid cylinders, i.e., the exterior of the monopile, and studies on moonpool fluid behavior has provided insights into the

interior fluid behavior in monopiles. Further investigation is required to comprehensively understand how to integrate the knowledge of both of these, as well as the behavior around sharp edges.

The hydrodynamic behavior of hollow monopiles can also be compared to that of moonpools, structures with enclosed water columns that have similar fluid dynamics. By looking into the equations used for moonpools [21], we can identify how force responses in hollow monopiles align with typical moonpool dynamics, especially in terms of resonance modes and forces. Moonpools are known for inducing unique hydrodynamic phenomena which impact forces and stability. These include resonant pumping, which is the up and down movement of the inner water column, sloshing, which is the side to side movement of the inner water column and vortex generation, which occurs when fluid flow separates abruptly from a sharp edge like the thin wall of the monopile, creating rotating regions of fluid due to sudden changes in pressure and velocity. The next section elaborates on the main hydrodynamic factors affecting a circular moonpool and the methodology applied in calculations.

2.3.2. Resonance Modes and Free Surface Dynamics

Large-diameter hollow monopiles are prone to internal resonance modes, which are crucial to consider during lowering operations. Two types of resonance are expected: sloshing modes, characterized by lateral oscillations of the inner water surface, and piston mode, where the water column oscillates vertically. Both of these modes are influenced by the dimensions of the structure and the frequency of incoming waves. Understanding these resonances is important, as they can amplify the hydrodynamic forces acting on the monopile and affect the lowering operation. The equations in this section are taken from Bureau Veritas' guidelines on moonpools [21].

Piston Mode

The piston mode arises from the vertical oscillations of the water column within the moonpool, which can occur when the wave period aligns with the natural period of the moonpool. This resonance causes the water column to oscillate vertically, sometimes exceeding the moonpool's upper boundary. The natural period T_m for a circular moonpool of constant cross-section is calculated using equation 2.11.

$$T_m = 2\pi \sqrt{\frac{h}{gKA}} \tag{2.11}$$

where h is the height of the water column in the moonpool, A is the cross-sectional area, g is the gravitational acceleration, and K is a factor based on the shape of the moonpool. For a circular cross-section, K is approximately 0.479.

The risk of resonant pumping mode is to be considered when the amplification factor, which is the ratio of the natural period of the moonpool to the wave peak period, is between 0.6 and 1.3. The height of the water level in piston mode can be calculated by multiplying this amplification factor with the wave height of the incoming wave [22].

To predict the amplitude of piston mode oscillations inside the moonpool when subject to wave action, the response amplitude operator can be calculated using equation 2.12 [23].

$$RAO = \frac{1}{\sqrt{(1-(\omega/\omega_0)^2)^2 + (2\zeta\omega/\omega_0)^2}} \tag{2.12}$$

The height of the water level in piston mode can be calculated by multiplying this RAO with the wave height of the incoming wave.

Sloshing Modes

Sloshing can occur in moonpools when the natural periods in the longitudinal or transverse directions resonate with the vessel's pitch or roll periods. For a circular moonpool, the resonance period T_n for sloshing modes can be estimated by equation 2.13

$$T_n = \frac{2\pi}{\omega_n} \tag{2.13}$$

where ω_n is the moonpool natural angular frequency in rad/s, which is influenced by the height of the water column h, gravity g, and the mode number n through equation 2.14. These natural frequen-

cies are critical for predicting sloshing-induced loads on the moonpool boundaries, particularly under conditions where the vessel motions match sloshing resonance.

$$\omega_n^2 = g\lambda_n \frac{1 + J_n + tanh(\lambda_n h)}{J_n + tanh(\lambda_n h)} \tag{2.14}$$

Where J_n is obtained from figure 2.2, in which the lower curve is for mode 1 and the upper curve for sloshing mode 2.

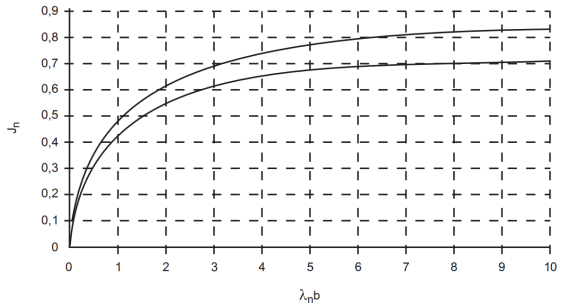

Figure 2.2: J_n curve [21]

Hydrodynamic Loads on Moonpool Structure
To mitigate the structural loads from resonant pumping, it is necessary to calculate the maximum pressures acting on the moonpool walls. For resonant pumping, the pressure p_{pump} at a height z from the bottom can be estimated with equation 2.15

$$p_{\text{pump}} = \rho g(D - z) \tag{2.15}$$

where D is the total height of the moonpool. This pressure estimate can be combined with other loading criteria for structural assessment under pumping and sloshing modes.

Bureau Veritas' guidelines [21] state: 'when the risk of sloshing cannot be excluded, the maximum sloshing pressure determined through direct calculations, model tests or other recognized approaches may be taken into account for the checking of moonpool boundaries', without stating an expression for sloshing loads.

2.4. Scaling in Wave Tank Experiments

Experiments for monopile analysis require accurate scaling to ensure that observed hydrodynamic behavior translates realistically to real-world conditions. Generally for wave tank testing, the Froude number, Reynolds number and Keulegan-Carpenter number are taken into account. They are non-dimensional numbers, often used for scaling in experimental research.

The Froude number is a dimensionless parameter that compares the inertial forces to the gravitational forces. It ensures that the ratio between inertial and gravitational forces is the same in both the model and the prototype. This is particularly useful for studies involving free surface flows. Maintaining the same Froude number ensures the correct wave patterns and behaviors in the model and is suitable for analyzing phenomena where gravity is the dominant force, such as wave-structure interactions.

The Reynolds number is another dimensionless parameter that compares inertial forces to viscous forces. Sticking to the same Reynolds number ensures that the flow regime (laminar or turbulent) is the same in both the model and the prototype. It is particularly important for studies involving viscous flows and boundary layers. The Reynolds number preserves the flow characteristics, such as turbulence and boundary layer behavior and is crucial for accurate representation of viscous effects in the model. Therefore, it is ideal for analysing phenomena where viscous forces are significant, such as drag and flow separation.

To maintain a constant Reynolds number while scaling down the geometric dimensions (D and L), the flow velocity (U) must be increased. Employing Reynolds number scaling typically results in larger

model structures and higher flow speeds, which pose challenges regarding the dimensional forces on the model and the test apparatus, the capacity of the test facility, and associated costs.

Scaling realistic offshore waves using the Reynolds number with a geometric scaling factor of 1/30 results in wave conditions that the wave maker in the wave tank cannot reliably reproduce. This limitation significantly impacts the accuracy and reliability of the scaled-down experimental conditions.

Moreover, this research focuses on the effects of the free surface rather than viscous effects. Scaling realistic offshore waves using Froude numbers with the same geometric scaling factor of 1/30 produces wave conditions that the facility's wavemaker can reliably generate. Consequently, model scaling based on the Froude number was chosen for this experiment.

The Keulegan-Carpenter (KC) number is a dimensionless number describing the relative importance of drag forces over inertia forces for objects in oscillatory fluid flow, such as waves. In a sinusoidal wave, the KC number can be calculated according to equation 2.16. For deep water waves, the ones assessed in this research' experiment, the amplitude of the wave can be used to calculate the KC number as well.

$$KC = \frac{u_a \cdot T}{D} = \frac{\zeta_a \cdot T}{D} \tag{2.16}$$

For relevant offshore waves for this problem, the KC number has a low value. For low values of KC (KC<3) the inertia force is dominant. This means the flow does not travel far enough to the cylinder diameter to generate much of a boundary layer or vortices.

The low KC number indicates that inertial effects, such as the movement of the inner water surface, are more dominant in this problem than viscous effects. Considering that this research focuses on the effects of the free surface rather than viscous effects, and scaling realistic offshore waves using the Froude number produces wave conditions that the facility's wavemaker can reliably generate, the conclusion is drawn again that model scaling based on the Froude number is most suitable for this experiment.

2.5. Summary

This chapter reviewed the relevant literature on the hydrodynamic behavior of structures similar to monopiles, focusing on solid vertical cylinders and moonpools. The Morison equation was introduced as a foundational approach for predicting hydrodynamic forces on solid cylinders, highlighting its limitations for the current problem, particularly for short-wave conditions and surface-piercing hollow structures. Diffraction theory and numerical tools like ComFLOW were identified as complementary approaches, especially for scenarios where wave diffraction dominates.

Moonpool hydrodynamics were explored to understand the fluid behavior inside hollow structures with free water surfaces. Key phenomena, including sloshing and piston-mode resonances, were discussed, emphasizing their sensitivity to geometric and environmental factors. These insights provide a foundation for understanding the complex fluid-structure interactions inside monopiles, especially given their larger diameters and thin-walled construction compared to traditional moonpools.

Although both solid cylinders and moonpools offer valuable theoretical frameworks, monopiles differ due to their unique combination of external wave forces and internal water dynamics. Unlike moonpools, where damping is influenced by substantial surrounding structural volumes, monopiles feature sharp edges and thin walls, likely intensifying localized flow phenomena and resonant behavior. This highlights the need for tailored analytical and experimental approaches to capture the interplay of external forces, internal resonances, and viscous effects specific to monopiles. Viscous effects, such as flow separation and damping at sharp edges, are important for understanding how monopiles interact with waves. However, this research focuses on inertial effects because they are governing for the hydrodynamic forces during lowering operations.

In summary, while the theories and methods developed for solid cylinders and moonpools provide a baseline, they are not able to fully and accurately model large diameter monopiles during vertical lowering operations.

3

Experiments

This chapter describes the experiment that was conducted to measure hydrodynamic forces on the monopile. Details on the wave tank setup, test conditions, and measurement techniques are provided, ensuring the consistency and reliability of the results.

3.1. Introduction

The experiments aim to assess whether hydrodynamic forces on the monopile can be accurately predicted using existing models for solid cylinders and moonpools, as monopiles lie at the intersection of these structures. The study explores the dynamics of the free surface within the monopile, including resonance modes (piston mode and sloshing modes), and how different drafts during the lowering procedure influence these forces.

The experimental setup simplifies the system to a large diameter hollow surface-piercing cylinder, subjected to incoming monochromatic waves, to quantify the wave-exciting forces and behavior of the inner water surface. Three distinct drafts have been selected to resemble the various drafts during the lowering procedure of the monopile.

A simple schematic of the experimental setup is shown in figure 3.1.

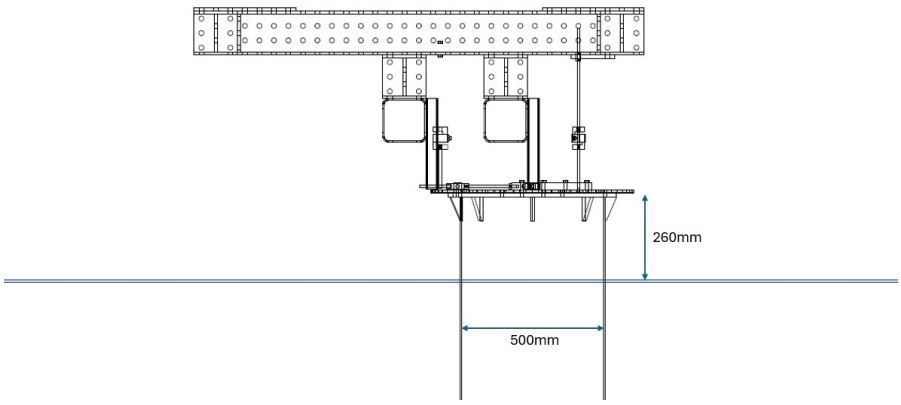

Figure 3.1: Experimental Setup

The primary objectives of the experiments are to create controlled conditions using monochromatic waves that resemble waves in a realistic offshore wave spectrum, to measure the forces and moments acting on the monopile model at distinct drafts in the lowering procedure for these waves, and to observe and quantify the free-surface behavior inside the monopile model for these waves at distinct drafts in the lowering procedure.

The secondary objectives of the experiments are to create controlled conditions using monochromatic waves that induce the expected resonance modes within the inner water column of the monopile

model. To measure forces and moments acting on the monopile model during induced resonance modes of the free-surface, for three different drafts and to observe and quantify the free-surface behavior inside the monopile model during induced resonance modes.

3.2. Experimental Setup

For dimensional reference, the XXL monopile from Seawind [24] has been utilized. According to International Towing Tank Conference guidelines [25], both the model and full-scale structures must maintain identical shapes, ensuring the ratio of diameter to length (D/L) remains constant for a circular cylinder. The dimensional scale factor of choice is 1/30.

The model used in the wave tank has minor deviations from the intended scale factor for wall thickness, due to the constraints of the materials available the wall thickness of the model is 4mm instead of 5mm. These deviation is assumed to be negligible and to not affect the experiment's results, as the purpose it is still a thin-walled model. The dimensions of the full scale and model scale monopile for this project are displayed in table 3.1. Note that the dimensions of the full scale are given in meters while the dimensions of the model scale are in millimeters. The designed model was initially supposed to have 30cm of freeboard in the setup. Building the setup it was found that it is actually just 26cm of freeboard, meaning the three measured drafts were 0.34m, 0.94m and 1.54m.

Dimension	Full Scale	Model Scale
Diameter	15 m	500 mm
Full Length	135 m	2200 mm
Water Depth	75 m	2200 mm
Wall Thickness	0.15 m	4 mm
Draft 1	9 m	340 mm
Draft 2	18 m	940 mm
Draft 3	45 m	1540 mm

Table 3.1: Dimensions full scale monopile

The experiments will be conducted in a wave tank. The tank that is used is Towing Tank No. 1 in the Mechanical Engineering building of Delft University of Technology. The dimensions of this tank are displayed in table 3.2

Length	142.00 m
Width	4.22 m
Water depth	2.30 m
Wavemaker type	Flap type, electronic/hydraulic
Wavelength	0.30 - 6.00m, regular/irregular

Table 3.2: Towing Tank No. 1 (TU Delft) Specifications

The tank water depth is larger than the model itself because there is no intention of putting the model all the way down to the bottom of the tank. This is because no large forces are expected in the last part, as particle velocity is lower at larger depths. Additionally, in a real offshore monopile installation operation, the monopile will likely be constrained in its movements close to the seabed by use of guides or catchers, so less attention has to be paid to its hydrodynamic forces as the forces are partially absorbed by the guides.

A schematic of the experimental setup is displayed in figure 3.2. The positive x-direction is defined in the direction of the waves. The setup was built using steel H-beams of 0.15 x 0.15 m cross-section, creating a stiff structure. Three load cells of the type H3-C3-50kg-3B by Zemic were used for the x- and y-direction force transducers and for the z-direction another three load cells were used, these ones of type H3-C3-150kg-3B by Zemic. A PMMA cylinder was used as monopile model. The roundness of the cylinder was checked and a maximum difference of 0.5% in diameter was found. The cylinder has a smooth surface.

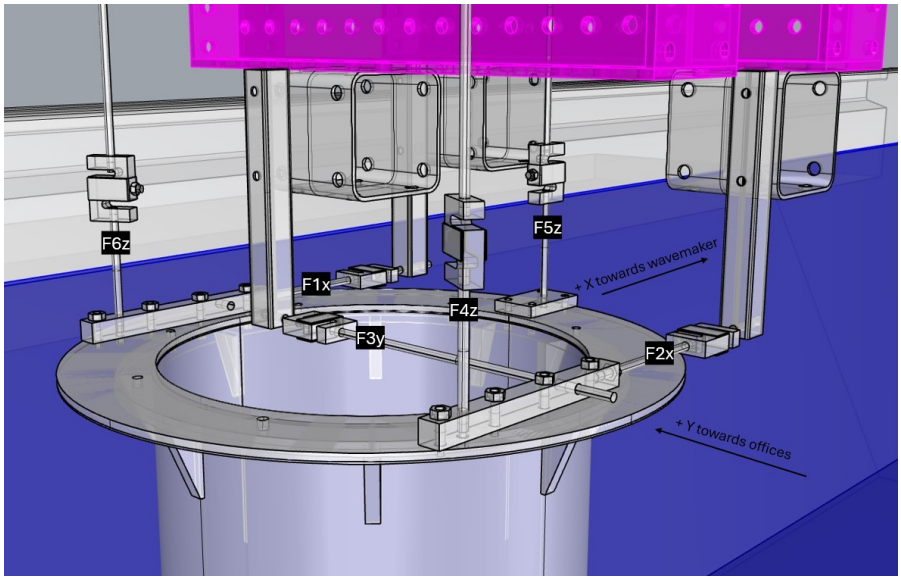

Figure 3.2: 3D image of Experimental Setup in Rhinoceros

A 2-dimensional drawing of the 6 DOF frame that was designed specifically for this experiment is shown in figure 3.3. The steel frame was treated with a metal paint to protect it from corrosion.

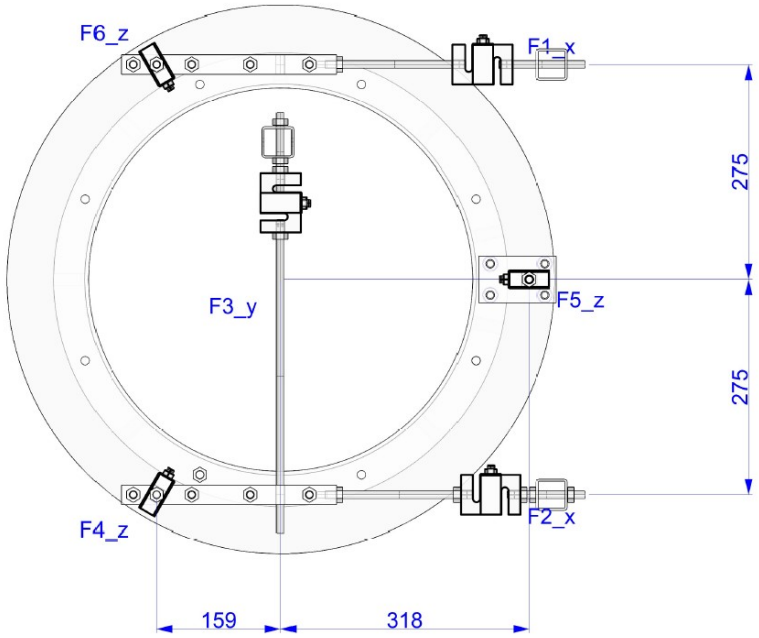

Figure 3.3: Configuration of the 6 DOF Force Transducer Frame, dimensions in millimeters

To obtain the necessary data, the undisturbed wave need to be measured, the height of the inner water column of the cylinder and the forces and moments on the cylinder in waves. Installing a camera next the cylinder allows for visual review of the experiments and to capture any unexpected events.

To measure the undisturbed waves we used an acoustic sensor to measure the water height a couple meters before interference with the model. Another acoustic sensor was placed along the center line of the model further towards the side of the wave tank. To measure the wave elevation inside the monopile, aluminium strips were glued to the inside of the model. It was found that using conventional wave gauges inside the monopile model would influence the inertia properties of the model too much.

Multiple strips are required for measuring any irregular behavior along the water surface and to ensure reliable measurement in case one of the strips is inaccurate, therefore three strips were used, one at the front of the cylinder, one at the back, and one at starboard side to be able to measure swirled sloshing if it might occur. The measurement frequency of all the sensors in the experiment was 100 Hz.

Because of the shape of these strips, a thickness less than 0.5mm, the flow separation effects of the strips is assumed to be negligible. Since they are stuck to the walls of the cylinder, wall effects do have to be taken into account. A possible outcome of this would be that the measured water level inside the cylinder is slightly higher than the true level in the middle of the column, because some water will ”stick” to the strip. This is due to capillary effects and surface tension. When water comes into contact with a solid surface, intermolecular forces cause the water to adhere to the surface, creating a small rise (or depression) at the contact point [26]. The formula to calculate capillary rise is given by equation 3.1.

$$h = \frac{2\gamma \cos\theta}{\rho g R} \tag{3.1}$$

Where h is the height of the capillary rise, γ is the surface tension of the water at 20 degrees (=0.072 N/m), θ is the contact angle, ρ is the density of the water (=998 kg/m^3), g is the acceleration due to gravity and R is the radius of the cylinder or capillary tube.

The material of the cylinder is PMMA and that of the water level measuring strips is aluminium. These materials are considered hydrophilic, meaning the water tends to spread out more. To account for this effect, the contact angles are reduced to 70 degrees for both PMMA and aluminium [27] in equation 3.1. This results in a capillary rise of approximately 0.01mm for this model. The smallest wave that is tested is 0.033 meters high, meaning this will influence the results by maximum 0.03%.

3.2.1. Calibration of Sensors

Additional matter to take into account is the calibration of some sensors. All the wave load cells are subject to small errors. They can be calibrated by using a setup in which the actual force on the load cell is known, whilst measuring the signal output of the load cell. This calibration was executed for all six load cells and they were calibrated for both strain and stress forces. From this calibration, for each load cell a calibration factor is obtained and the signal is multiplied by this factor to ensure the right output in the data. The average error of the load cells was 0.15%

For the 6 DOF frame, it is known that due to the geometry of the setup, some of the force in one direction will be taken in by the force transducers in other directions. To find out the contribution of the other transducers in each direction, a calibration was done in which the 6 DOF frame was put under tension by a known force in the x- and y direction and weights were used for the z-direction. From this calibration it was found that for the x-direction, the other load cells take in 0.9% of the total force. For the y direction, the other load cells take in 0.1% of the total force, and for the z direction, the load cells take in 0. 3% in the other directions.

For the wave measurement strips inside the cylinder, a calibration has also been executed, where the true water level was measured visually through the grid on the model, while measuring the output signal of the water level height strips. Through this calibration it was found that the errors between the true and measured water level are maximum 2%.

3.2.2. System natural frequencies

In any experimental setup, the natural frequencies of the system are a critical factor that can significantly influence the behavior of the structure under various loading conditions. Natural frequencies are intrinsic properties of the system that depend on mass, stiffness, and boundary conditions.

For this experiment, it is important to identify the natural frequencies of the system before introducing wave conditions. This will allow us to distinguish between the natural response of the system in still water and any resonance effects induced by the monochromatic waves. In doing so, we can ensure that the observed resonant behavior in the presence of waves is due to the wave-induced forces rather than an inherent property of the system in still water.

To achieve this, a decay test will be conducted on the system in a still-water environment, absent of wave influences. In this test, the structure will be excited by an external impact. This impact will

displace the system, causing it to oscillate at its natural frequencies. The subsequent decay of these oscillations over time will be recorded.

The data collected from this decay test is analyzed using a Fast Fourier Transform (FFT), which converts the time-domain signal into the frequency domain. This transformation allows us to identify the dominant frequencies at which the system naturally oscillates. These frequencies are the natural frequencies of the structure in its current experimental setup.

The natural frequencies obtained for each draft with decay tests conducted in three directions are displayed in table 3.3.

Decay test	Draft 1 = 0.34m	Draft 2 = 0.94m	Draft 3 = 1.54m
in x-direction	0.64Hz, 1.38Hz, 8.47Hz, 11.4Hz	4.1Hz, 21.6Hz	2.6Hz, 12.4Hz
in y-direction	8.5Hz, 8.6Hz, 12.1Hz	4.2Hz, 23.5Hz	2.8Hz, 13.7Hz
in z-direction	1.39Hz, 100Hz	1.39Hz, 100Hz	1.38Hz, 19Hz, 100Hz

Table 3.3: Natural Frequency Responses obtained from Decay Tests in Three Directions

By conducting this decay test, the natural frequencies of the system can be accurately identified. This information is crucial for interpreting the results of the wave-induced tests that follow, as it allows to clearly distinguish between the natural vibrational modes of the structure and the resonant frequencies that may be triggered by external wave forces. For instance, if the system's natural frequencies align with the frequencies of the incoming waves, the structure could experience resonance that is independent of the hydrodynamic behavior being studied. This could lead to misleading conclusions about the behavior of the monopile. By conducting a decay test in still water to identify the natural frequencies of the setup, we can establish a baseline for comparison. Understanding this distinction is vital for accurately assessing the hydrodynamic behavior of the monopile and for ensuring that the observed phenomena are truly representative of the conditions that the structure would encounter in a real marine environment and can confidently be assigned to the monopile's specific hydrodynamic behavior, such as piston or sloshing modes. This step is especially important when investigating resonance modes, as these are a key focus of this study.

3.3. Test Plan

To be able to investigate the hydrodynamic forces of large-diameter monopiles in marine environments, realistic offshore sea states have been selected. This approach ensures that the experimental conditions closely mimic the actual conditions these structures would encounter in the ocean. By choosing representative sea states, the study aims to provide accurate and relevant insights into the performance and challenges faced by monopiles in real-world scenarios. Rather than trying to induce resonance modes, the goal is to use real offshore scenarios to determine if resonance modes are likely to occur during the installation of monopiles. Using the data provided in (Beels, 2007) 16 monochromatic waves have been selected. Even though in a realistic sea state currents would also be present, this study focuses on the influence of the waves on the hydrodynamic forces. To be able to capture the effects of waves most clearly, current was not present in the experiment. Each monochromatic wave and draft combination is repeated between two to four times to obtain consistent results.

3.3.1. Wave Modeling

Rather than using a spectrum of waves as it is in the real world scenario, for the experiment monochromatic waves were selected to provide more clear results and to make the results of the experiment easier to compare to existing predicting methods, as the waves are predictable and are the maximum condition in cases of resonance like piston mode and sloshing. Out of the sixteen selected monochromatic waves, twelve are representative of typical North Sea wave conditions, specifically chosen to match the water depths corresponding to the dimensions of the large-diameter monopile investigated in this research.

The parameters of the monochromatic waves investigated at world scale vary from 1m to 3.2m wave height and 5.5s to 8s periods, having wave lengths between 47.3m and 100m. The four remaining selected monochromatic waves have been chosen to specifically induce the expected resonance modes at certain frequencies and do not resemble North Sea installation conditions. These waves are specifically designed for the secondary objectives of this experiment: to induce resonance modes and measure the forces during resonance. The parameters of these waves vary from 1.5m to 3.6m wave heights and 9s to 14s periods, having wave lengths between 126m and 306m.

The experimental program displayed in table 3.4 was performed for 8 different wave periods and four different wave height to wave length ratios (wave steepness): $H/\lambda = 0.021, 0.025, 0.032, 0.012$ where H is the wave length and λ is the wavelength from the deep water dispersion relation. The experiments were repeated at least once and documented with a video camera. Prior to the experiment, a wave calibration series was performed without the model.

Twelve waves are divided into four groups of the same wave length (1.57m to 3.33m) with in each group three different wave heights, 'low', 'medium' and 'high'. The four 'extra' waves in the full right column have increasing wave length, while steepness is kept the same.

Wave	Low-1.57m	Medium-1.57m	High-1.57m	Extra-4.2m
H	0.033m	0.040m	0.050m	0.050m
λ	1.574m	1.574m	1.574m	4.216m
Steepness	0.021	0.025	0.032	0.012
Wave	Low-1.87m	Medium-1.87m	High-1.87m	Extra-5.2m
H	0.040m	0.048m	0.060m	0.062m
λ	1.874m	1.874m	1.874m	5.204m
Steepness	0.021	0.025	0.032	0.012
Wave	Low-2.55m	Medium-2.55m	High-2.55m	Extra-6.3m
H	0.054m	0.065m	0.081m	0.075m
λ	2.550m	2.550m	2.550m	6.297m
Steepness	0.021	0.025	0.032	0.012
Wave	Low-3.33m	Medium-3.33m	High-3.33m	Extra-10.2
H	0.071m	0.085m	0.106m	0.121m
λ	3.331m	3.331m	3.331m	10.201m
Steepness	0.021	0.025	0.032	0.012

Table 3.4: Monochromatic waves used in the experiment

3.3.2. Data Processing

For this research, hydrodynamic forces in all directions have to be obtained for various frequencies as these give insights in the response of the monopile subject to incoming waves that are likely to occur during a monopile lowering operation offshore. Section 4.1 in the next chapter will discuss what the data obtained from the experiment looks like and how the signals are processed to get to the final results.

3.4. Summary

This chapter described the experimental setup and methodology used to investigate the hydrodynamic forces and inner water behavior of a large-diameter monopile during lowering operations. The experiments were conducted in a wave tank, using a scaled model of the monopile with key drafts selected to represent different stages of the lowering process.

The setup was designed to capture wave-induced forces, moments, and inner water behavior, including resonance effects like piston and sloshing modes. Monochromatic waves were chosen to simplify the analysis and highlight specific responses. Froude number scaling ensured accurate wave behavior, though viscous effects were not fully replicated. Calibration of sensors and decay tests for natural frequencies helped to minimize measurement errors and distinguish wave-induced phenomena from system-induced resonance responses.

The experiments provide valuable measurements of hydrodynamic forces and moments, as well as insights into the behavior of the inner water column. This data is essential for understanding the dynamic response of monopiles during offshore operations and the basis for the analysis of the hydrodynamic forces, moments and inner water column resonance behavior in the next chapter.

4

Results

4.1. Introduction

This chapter presents the experimental results obtained from wave tank tests conducted on a large-diameter monopile model. The aim of these experiments was to analyze how the monopile interacts with incoming waves in terms of hydrodynamic forces, moments, and inner water level behavior during the monopile's vertical lowering operation. To achieve this, model tests were carried out at three different drafts for various incoming monochromatic waves.

To measure the forces and moments acting on the monopile, the model was suspended from a frame equipped with six force transducers. These transducers measured the forces in three orthogonal directions. The configuration of the frame was shown in the previous chapter in figure 3.3.

Using the measured signals from these transducers, the forces and moments in the relevant directions can be calculated using the following equations.

$$F_x = F_{1x} + F_{2x} \qquad M_x = (F_{4z} - F_{6z}) \cdot 0.275\,\text{m}$$
$$F_y = F_{3y} \qquad M_y = F_{5z} \cdot 0.318\,\text{m} - (F_{4z} + F_{6z}) \cdot 0.159\,\text{m}$$
$$F_z = F_{4z} + F_{5z} + F_{6z} \qquad M_z = (F_{1x} - F_{2x}) \cdot 0.275\,\text{m}$$

Figure 4.1 shows the time-domain signal of a complete measurement for wave 'Low-1.57m' on the model with draft 0.94 meter. This measurement captures the behavior of the model starting just before the moment the wavemaker started generating waves, lasting three minutes.

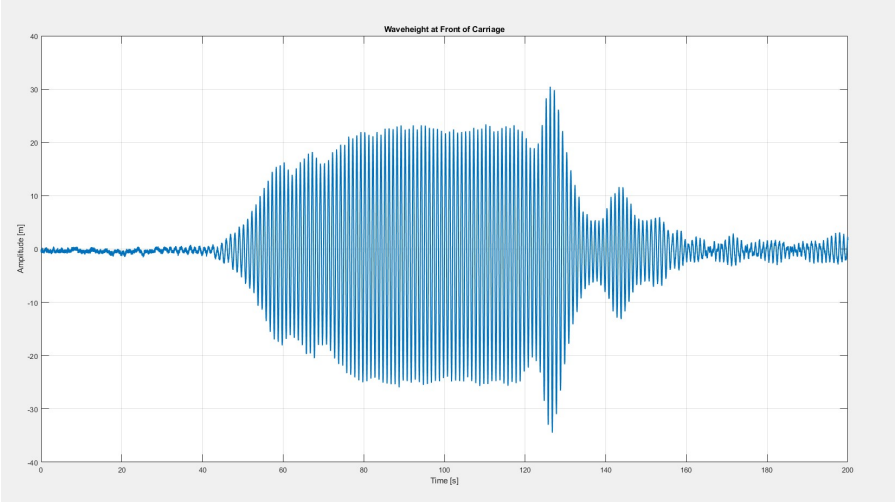

Figure 4.1: Full Time Domain Signal wave 'Low-1.57m' on draft 0.94m

At the start of the signal, the values are close to zero. The wavemaker starts to make waves and when they reach the model, the first wave amplitudes start to show in the data (around 50s). The wavemaker uses a ramp-up function to gradually generate the most accurate set of waves. The initial waves are therefore not used. In the middle portion of the signal (85s - 115s), the motion becomes harmonic, with a consistent amplitude for several wavelengths. This steady section was used to extract the data for further analysis. Toward the end of this steady section, the amplitude increases slightly before decreasing again (120s - 135s). This behavior is due to the settings of the wavemaker.

Later in the time signal, the amplitudes rise again (140s - 150s). This increase is caused by the first reflected waves already traveling back toward the model after hitting the wave tank's far end. These reflected waves are a natural part of the wave tank environment and the back and forward reflected waves are visible in the rest of the measured signal (150s - 200s).

The full signal is important for checking whether the force transducers are behaving as expected. After confirming that the transducers worked correctly, the data was trimmed to focus on the portion most relevant for analysis. Specifically, the data was trimmed to the middle section of the signal, where the motion was both harmonic and consistent. This ensures that only reliable and representative data was used for further processing.

Figure 4.2 presents an example of the trimmed time-domain signal for the Fx and My output of the sensors. The signal represents a smooth harmonic motion, which aligns well with the sinusoidal nature of the monochromatic waves. This harmonic behavior makes it suitable for analysis in the frequency domain using a Fast Fourier Transform (FFT). When performing an FFT, it is crucial to ensure that the system's eigenfrequencies do not interfere with the wave frequencies. Such interference could influence the results of the measurement and affect the interpretation of the measured forces and moments.

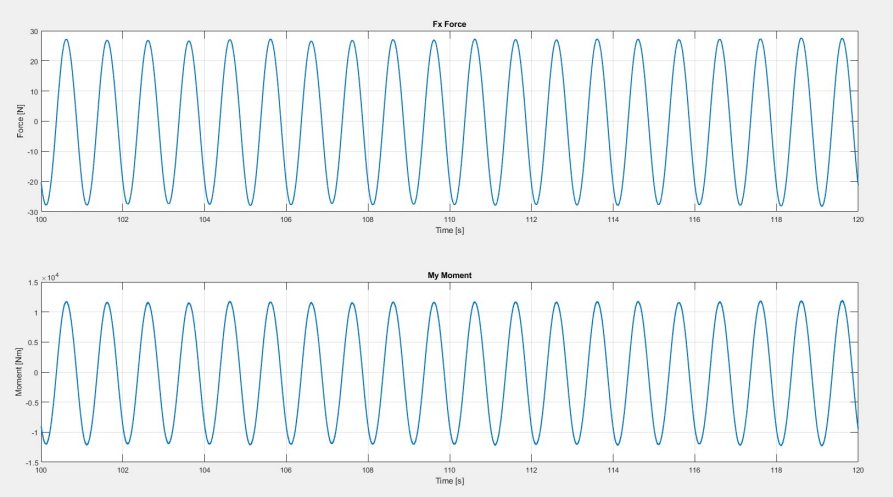

Figure 4.2: Harmonic signal for Fx and My for Wave 'Low-1.57m' on draft 0.34m

Figure 4.3 illustrates a typical FFT plot for the measured data of wave 'Low-1.57m' at three different drafts. In this case the wave frequency was 0.99 Hz which is clearly visible in the plot as the highest peak. Additionally, the eigenfrequencies of the system are marked on the plot for reference. These eigenfrequencies were determined experimentally by giving the whole system, so the model and the force transducer frame, a displacement in each of the three orthogonal directions and measuring the resulting free oscillations without any waves present. As visible in the figure, the eigenfrequencies do not interfere with the wave frequency. This means that the signal displayed is the response of the system to the waves solely. Figure 4.3 clearly shows where the peak is located, but not how the data is distributed. To be able to see this distribution better, a method called Zero Padding is used. An explanation of this method follows in the next paragraph.

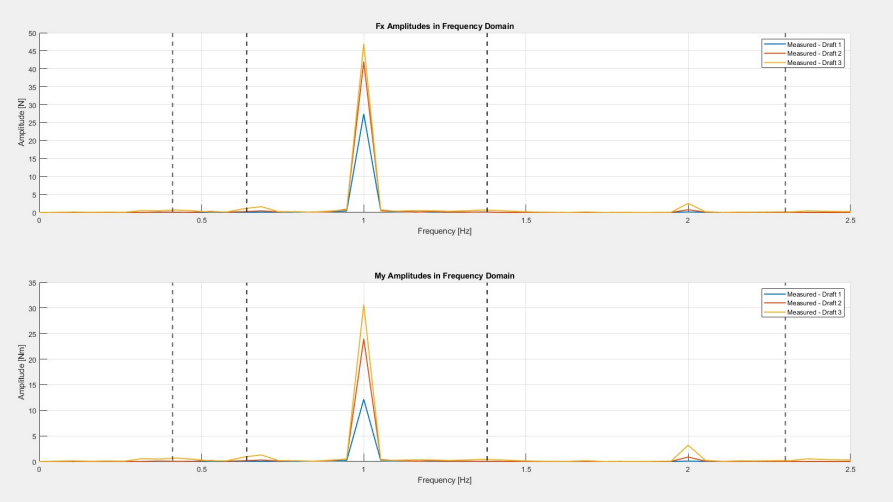

Figure 4.3: Fast Fourier Transpose Signal Without Zero Padding for wave 'Low-1.57m'

Zero padding involves extending the time signal with additional zeros before applying a Fourier Transform. Zero Padding enables you to obtain more accurate amplitude estimates of resolvable signal components[28]. This approach helps improve the resolution in the frequency domain, showing a clearer signal in the output without affecting the measured data itself. Figure 4.4 shows the data when Zero Padding was applied.

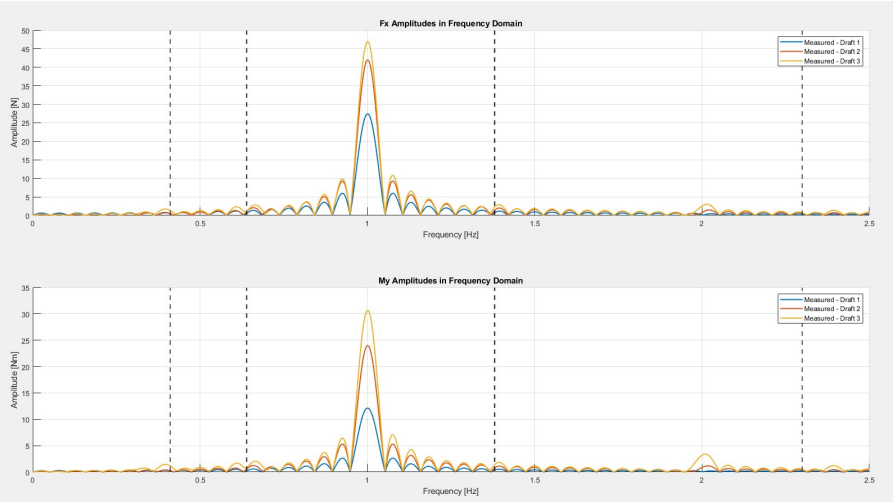

Figure 4.4: Fast Fourier Transpose Signal With Zero Padding of 10^7 zeros and system eigenfrequencies indicated by dotted lines for wave 'Low-1.57m'

It is important to note that the measurements have some minor deviations in their output for two reasons. Firstly, the force transducer frame is not hanging precisely horizontal. The angles were calculated during the calibration of the system. The force transducers in X direction had an angle offset of -0.009 degrees maximum to the Z-axis. The force transducers in Z direction had an angle offset of -0.005 degrees maximum to the X-axis, and the force transducers in Y direction had an angle offset of -0.005 degrees maximum with respect to the X-axis. The rods used in the mounting will partially transfer the force when they are a little bit strained orthogonal to their long axis. These offsets are found to be negligible for the goal of the experiment.

The steps described above, including signal trimming, harmonic motion analysis, and frequency-domain transformation using FFT with zero padding, were applied to all 16 wave conditions tested during the experiment for three drafts. The detailed data for each individual wave, including the processed time-domain signals and corresponding FFT plots, can be found in Appendix A.

4.2. Results: Forces and Moments

To summarize the results and highlight the trends observed across all 16 wave conditions, comparative plots were created. The most important plots are the ones for F_x and M_y, as these are the force and moment in the direction of the incoming wave. Figure 4.5 presents the peak forces (F_x) measured during the tests, normalized by wave height (H), as a function of wave frequency. Figure 4.8 does the same for the peak moments (M_y). This approach enables a clear visualization of the relationship between wave parameters and the hydrodynamic response of the monopile, such that direct comparison across wave conditions and drafts is possible. In these figures, there is a comparison being made between the measured data and the data analytically calculated using Morison's formula as described in Chapter 2. These comparative plots are created for forces and moments in all three orthogonal directions.

4.2.1. Force Analysis

The normalized Fx amplitudes are shown in figure 4.5. The theoretical values consistently exceed the measured data, particularly for shorter wavelengths.

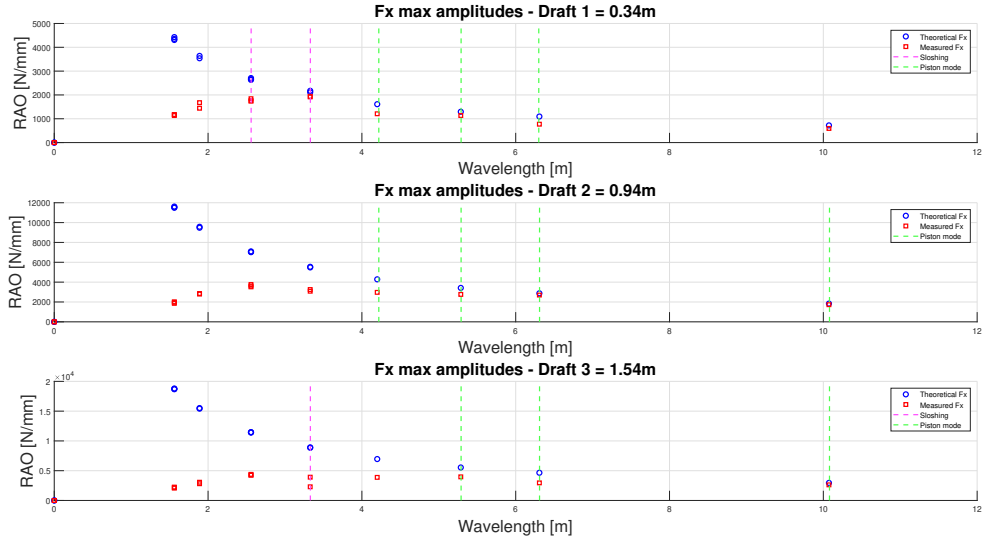

Figure 4.5: Fx amplitudes normalized by wave amplitudes

As figure 4.5 shows, the theoretical model generally predicts higher values for forces compared to the measurements, which may point to overestimation due to idealized assumptions that do not fully reflect the physical conditions in the wave tank. This discrepancy is particularly noticeable at shorter wavelengths, where measured values fall significantly below theoretical expectations. This is because these are based on the hydrodynamics of a slender cylinder, which implies that its diameter is small relative to the wave length. The method used is often usable as long as the diameter is 10 to 20 times smaller than the wave length. For the waves investigated, this is not the case. This was explained thoroughly in section 2.2.2.

For shorter wavelengths, the Morison equation becomes inapplicable because its assumptions no longer hold. In these cases, the wave interaction with the structure is dominated by diffraction effects, which the Morison equation does not account for. Therefore, diffraction theory or software like ComFLOW is required to accurately predict forces for these conditions.

In theory, the Morison equation is applicable only for wavelengths that are at least 10 times longer than the cylinder diameter. This trend is visible in the data, as the measured and theoretical values begin to converge for wavelengths around 5–6 m. This corresponds to approximately 10 times the diameter of the cylinder used in the experiment (0.5 m). For wavelengths shorter than this threshold, the limitations of the Morison equation become evident. From figure 4.5 we see that especially as the draft of the monopile increases towards draft 3 (1.54m), the convergence of the theoretical values and

measured values starts at wavelengths at least 10x larger than the diameter, whereas for lower drafts 1 (0.34m) and 2 (0.94m) the convergence is visible before this threshold. For draft 1 the Morison calculation already gives a reasonable prediction at wavelengths 6x larger than the diameter and for draft 2 at wavelengths 8x larger than the diameter. This means Morison method gets less applicable when monopile diameters increase, again showing the need for alternative modeling approaches, especially for increasingly large-diameter monopiles in offshore applications.

For reference purposes, comparing the theoretical expectations can still be useful. As the draft increases (from 0.34m to 1.54m), both the theoretical and measured forces rise, aligning with the expectation that deeper drafts interact more with incoming waves, generating stronger wave-induced forces, simply because the surface area is larger. However, the rate of increase is steeper in the theoretical values, suggesting possible damping effects in the experimental setup that the model does not account for.

The measured F_y component in figure 4.6 shows values that are higher than zero. Theoretically the value of F_y is expected to be zero if the undisturbed wave is traveling in x-direction. However, the experiments are done in a wave tank where reflections from the walls on the side are present, and furthermore it was established that the cylinder is not perfectly straight or perfectly circular causing small disturbances in the flow resulting in small force contributions over the y-axis. Along the different wavelengths and drafts there are some noteworthy results. At some specific wavelength and draft combinations the response F_y amplitudes suddenly increase more. For example at draft 1 for a wavelength of 3.33m the offset is twice the average offset of the other wave lengths. During the experiments for the waves with this wave length, piston mode and sloshing mode were observed, including sideways sloshing which is a possible explanation for the increased force in y-direction. Same goes for draft 3 for a wavelength of 10m where the maximum amplitude of the force in y-direction shows a response of 9.5N/mm while the expected force was zero. During the experiments of the wave with this wave length, a very clear piston mode was visible for draft 2 (=0.94) and draft 3 (=1.54). This is interesting, because in a piston mode one would not expect forces in y-direction. In section 4.3 we will dive deeper into the influence of the resonant modes on the hydrodynamic forces and explain these phenomena.

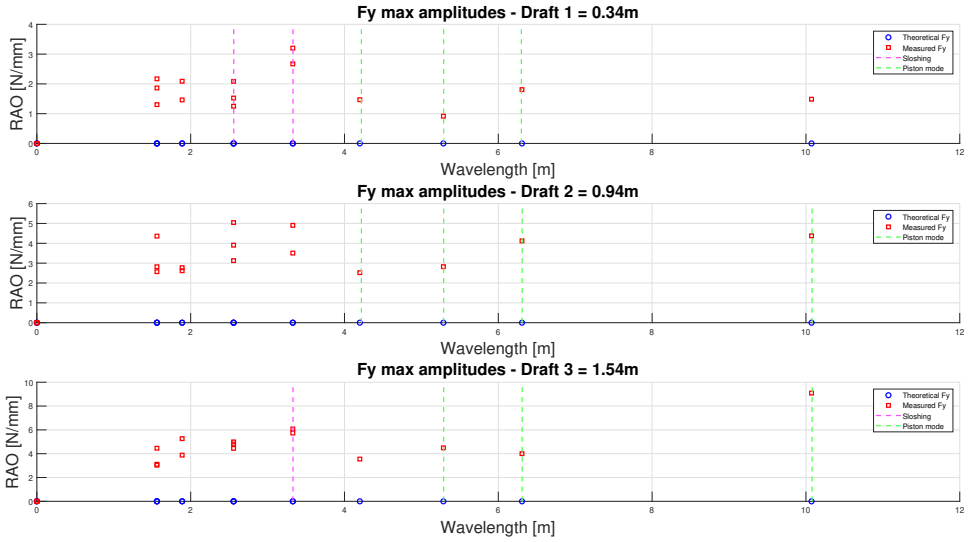

Figure 4.6: Fy amplitudes normalized by wave amplitudes

Fz shown in figure 4.7 follows a similar pattern, with measured values being higher than the theoretical force, which would be zero in z-direction, following the same analogy as described for the y-component of the force.

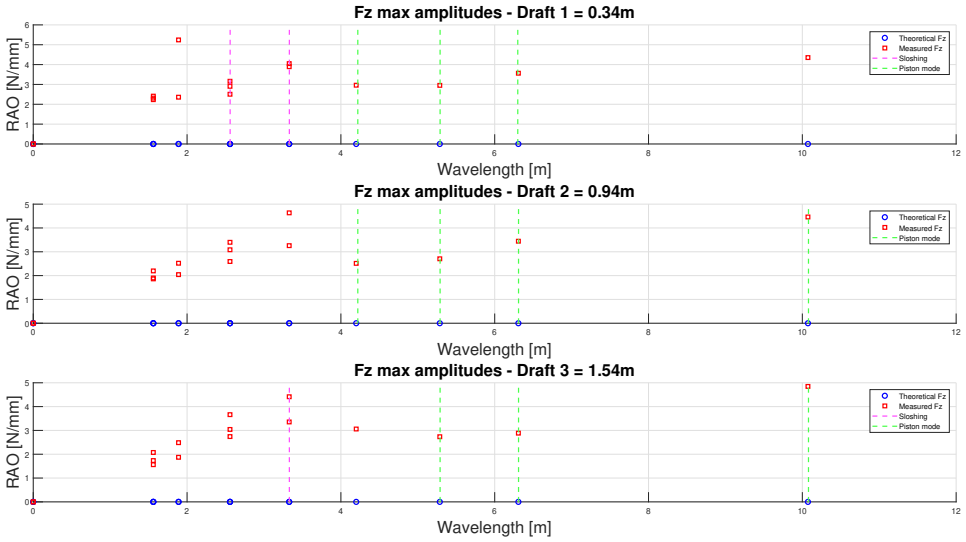

Figure 4.7: Fz amplitudes normalized by wave amplitudes

4.2.2. Moment Analysis

The moments also show a tendency for theoretical predictions to exceed measured values, particularly at shorter wavelengths and shallower drafts. The moments data is calculated from the force data, so it makes sense that measured values fall significantly below theoretical expectations since this happened for the force data because the Morison equation is not applicable for the short waves, as explained before in section 4.2.1. The theoretical moment around the y-axis also shows a steep increase in amplitude with draft, particularly at lower wavelengths, due to the larger interaction volume of the monopile with incoming waves. However, measured moments increase less steeply, suggesting some damping in the wave tank setup that is not reflected in the theoretical model.

Starting of by analyzing My, since this is the only direction in which a moment larger than zero is theoretically expected. For My as shown in figure 4.8, the theoretical predictions tend to exceed measured values, especially at the shorter wave, but the two converge more closely at longer wavelengths. This alignment for longer waves indicates that the theoretical model is more accurate for longer waves.

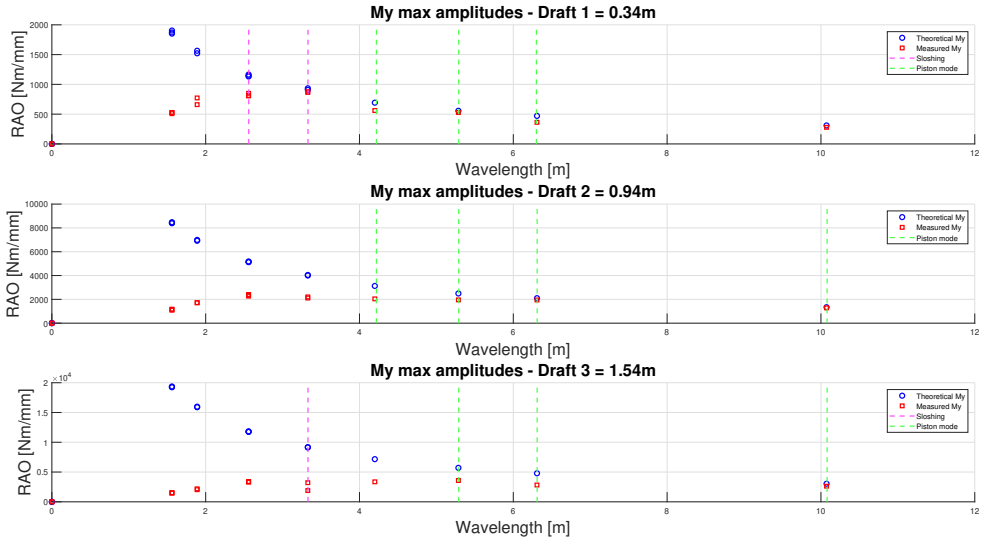

Figure 4.8: My amplitudes normalized by wave amplitudes

The comparison for moments around the x-axis are shown in figure 4.9. Theoretical values for Mx are zero, as for monochromatic waves in x-direction for a perfectly round cylinder, forces or moment in the orthogonal direction are not expected. These conditions are not very realistic for this experiment, as the hollow cylinder is not perfectly round and due to some movement in the water due to previous tests, the monochromatic waves might have some contributions in y-direction as well, next to their main direction along the x-axis. Furthermore, sideway sloshing was sometimes observed in the experiment. At frequencies where sloshing was expected, this sloshing sometimes turned into sideway sloshing due to the nature of the round geometry, causing forces in the y-direction and therefore moments around the x-axis.

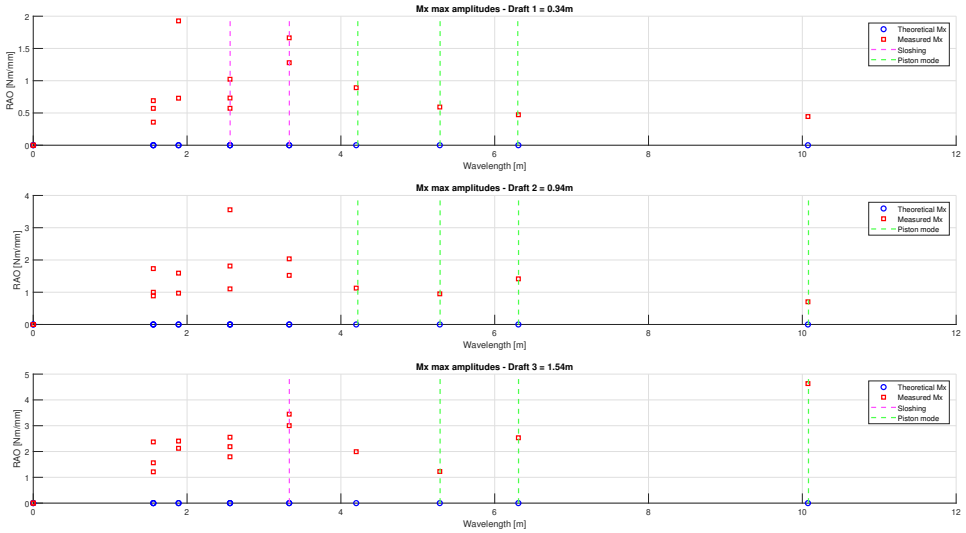

Figure 4.9: Mx amplitudes normalized by wave amplitudes

The Mz values in figure 4.10 also consistantly show that the measured forces are higher than the theoretical zero. Since the magnitudes of the moments induced by the waves is very low, with maximum 0.9 Nm/mm, the conclusion can be drawn that these discrepancies are caused by the experimental wavetank and monopile model environment.

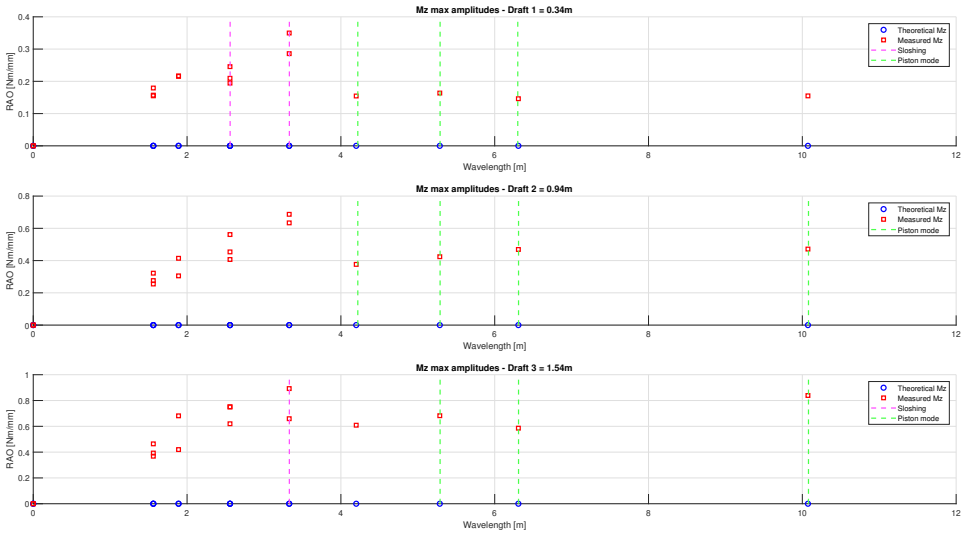

Figure 4.10: Mz amplitudes normalized by wave amplitudes

4.3. Results: Inner Water Column Behavior and Resonant Modes

The water level inside the cylinder was measured using water height measurement strips on the inside walls of the monopile model. The data measured is a time-domain signal for the three strips. There is noise on the signal, but the noise is the same for each sensor. The results of such measurement are displayed in figure 4.11 for wave 'Low-1.57m', the wave with lowest wave height and shortest wave length. Visibly, from the experiment, not much movement was observed for this wave. In the data we see that the sensors did measure some up and down movement for draft 1 (=0.34m) as a harmonic piston-like motion with an amplitude of 6mm, meaning the waterlevel inside the model went up and down as a whole at the frequency of the waves. For draft 2 (=0.94m) we see that the waterlevel measured for each strip at the same time stamp is different, meaning that at a time that the water level at the front of the model was highest, the water level at the back was lowest. The amplitude of the motion is small, around 4mm. For draft 3 (=1.54m) the waterlevel measured again shows a piston-like motion, where all the strips measured the same water level height at each timestamp. Again, the amplitude of this motion is small, around 4mm. For all of these observations the water level amplitudes inside the cylinder were small compared to the wave amplitude, which was 33mm for wave 'Low-1.57m'.

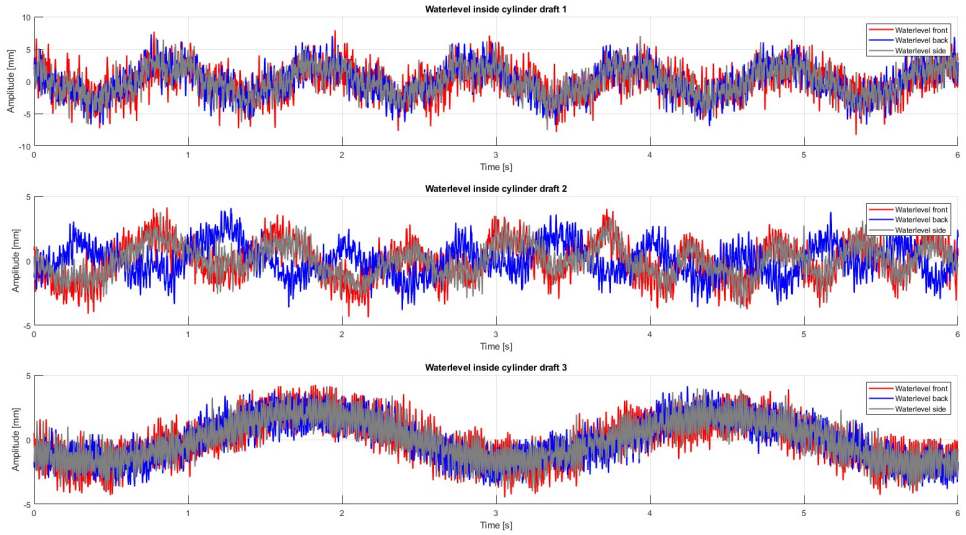

Figure 4.11: Time-domain measurements of water level strips for wave 'Low-1.57m'

Another time-domain measurement is displayed in figure 4.12, in this case for wave 'Medium-3.33m'. During the experiments for draft 1, side-way sloshing, sloshing and piston mode was observed. This shows in the data as we see a harmonic up and down motion for all the three strips in the front, back and side, but not all signals follow the same motion. It seems that both piston-mode and sloshing mode were induced at the same time, making the inner water column move up and down with an amplitude of 60mm, but also the water level sloshing in both x- and y-direction, extending the amplitude by max 40mm. For draft 2, there was no visible motion of the inner water column in the experiment, but the signal shown slight up and down movement with an amplitude of 8mm maximum. In the experiment with the draft 3 model, sloshing was observed. The sloshing pattern in x-direction shows clearly in the data as the front and back amplitudes have a harmonic motion with an amplitude of 5mm and opposite phase and the side amplitude is around zero. The sloshing motion of the free-surface was clearly visible in the experiment because the PMMA material is see-through. A picture of the phenomenon is shown in figure 4.13.

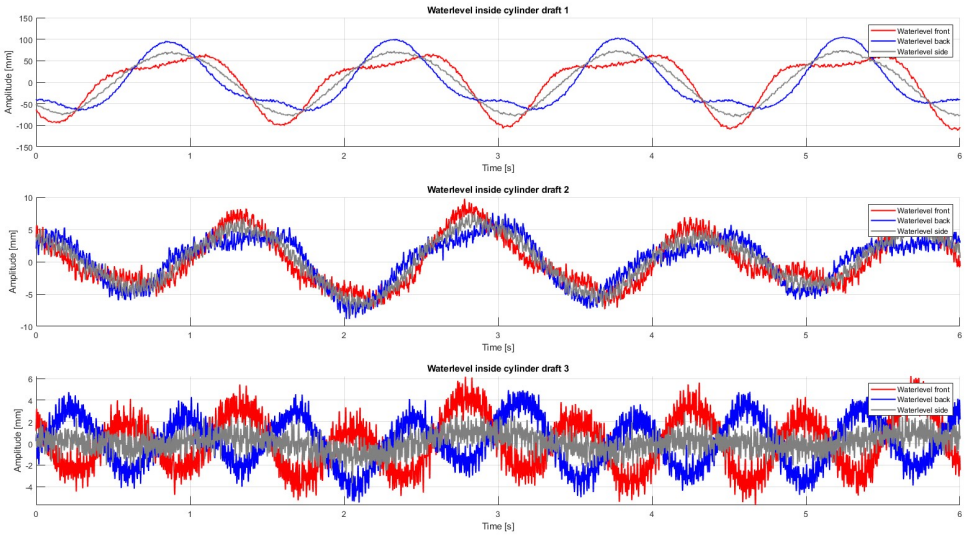

Figure 4.12: Time-domain measurements of water level strips for wave 'Medium-3.33m'

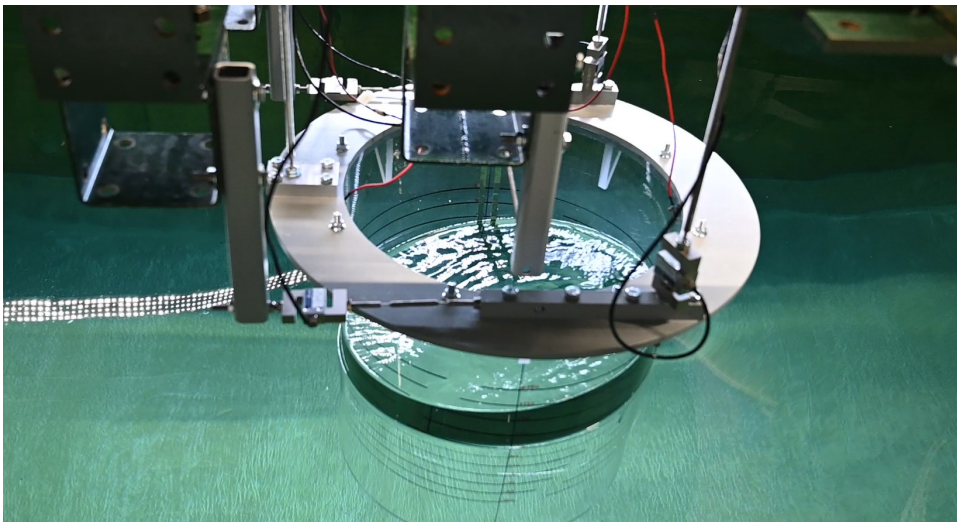

Figure 4.13: Sloshing in Experiment for wave "Medium-3.33m"

The third time-domain measurement that is highlighted is that of wave 'High-2.55m'. The data is displayed in figure 4.14. The data for draft 2 and draft 3 look a bit alike the data for wave 'Medium-3.33m' in figure 4.12, as the amplitudes are small but little motions are measured. The data we want to highlight from wave 'High-2.55m' in figure 4.14 is the data for draft 1, as it very clearly shows a piston mode, which was expected for this wave and draft combination.

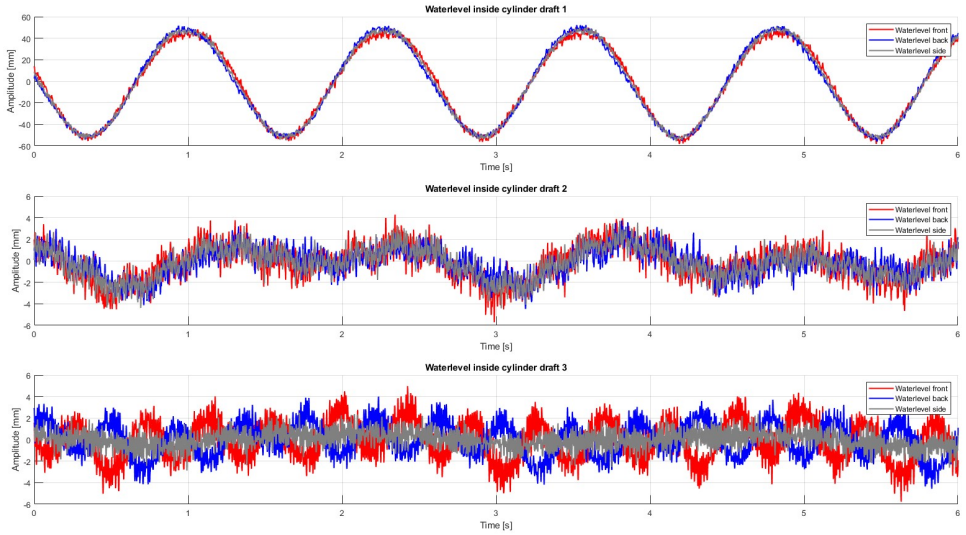

Figure 4.14: Time-domain measurements of water level strips for wave 'High-2.55m'

The piston-mode motion of the free-surface is shown in figure 4.16 and figure 4.15.

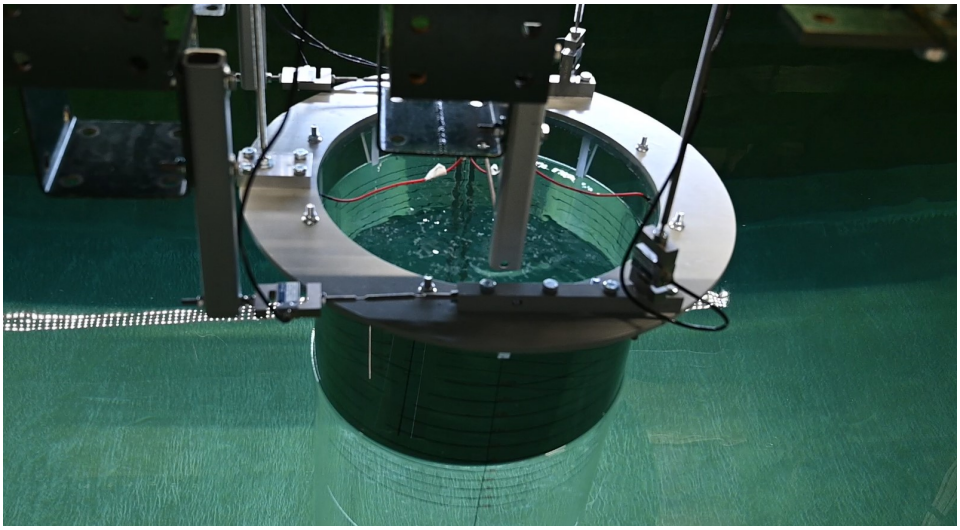

Figure 4.15: Observed Piston-Mode during the experiment for Wave 'High-2.55m' - upward

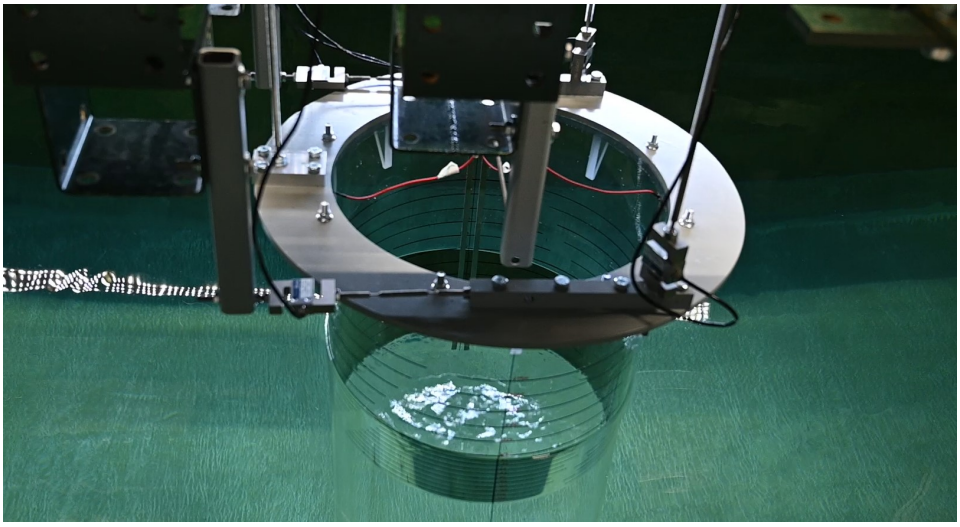

Figure 4.16: Observed Piston-Mode during the experiment for Wave 'High-2.55m' - downward

From these experiments, we are mostly interested in finding out whether the resonance theory for moonpools also applies for monopiles. Therefore the maximum water level amplitudes for moonpools subject to certain monochromatic waves was calculated using the method described in section 2.3.2 and is compared to the maximum water level amplitudes that were measured during the experiments. In equation 2.12 there is a damping factor included. The hydrodynamic damping is the sum of two contributions, wave radiation and viscous damping of the fluid. Both components are proportional to the relative velocity between the structure and the water. The hydrodynamic damping ratios recommended by the Germanischer Lloyd [29] are 0.11% and 0.15% for the radiation and the viscous damping respectively [30].

Using the same method as for the forces and moments, all the data was plotted in the frequency domain using FFT with zero padding. As seen from the time-domain measurements, the data contains noise but it is high-frequency noise, so it will not influence the data when it is transferred to the frequency domain. All of the maximum water level amplitudes of the monochromatic waves tested for monopiles are plotted in one figure, together with the expected theoretical water level amplitudes for moonpools. The water level amplitudes are normalized by the wave amplitudes. The normalized water level amplitudes are shown in figure 4.17 together with the analytically calculated water level amplitudes using moonpool theory [12] and the radiation- and viscous damping coefficients [30] added together as 0.26%.

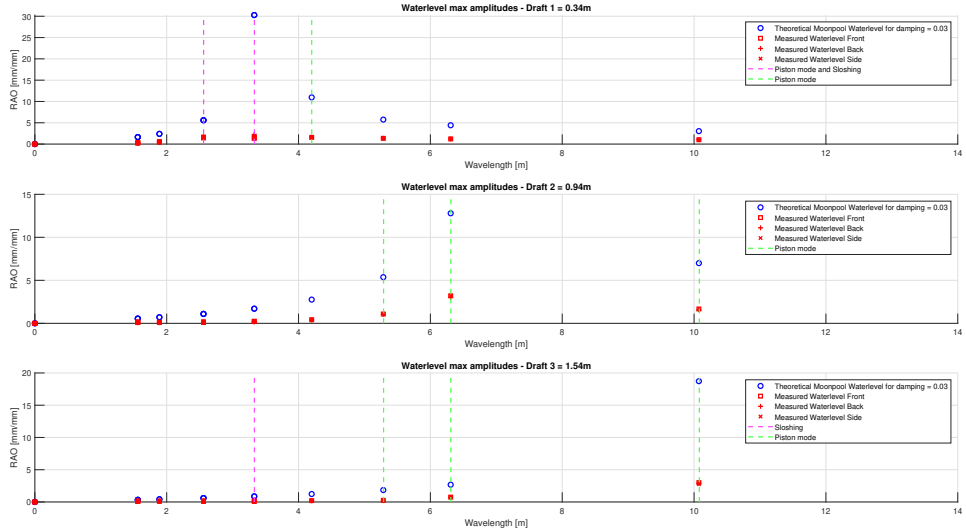

Figure 4.17: Water Level amplitudes normalized by wave amplitudes, damping ratio = 0.26%

From figure 4.17 can be concluded that the moonpool theory values are not a good prediction for the measured monopile values at this damping ratio. A better fit for the data was found when using a damping ratio of 2.2%. According to Kristiansen and Faltinsen [31] this discrepancy is mainly due to the effect of flow separation around the monopile's edges. The results are displayed in figure 4.18.

The first observation is that the moonpool theory values tend to exceed the measured data, except for some distinct wave lengths that are different per draft. The main take-away is that moonpool theory expects the inner water level to move up and down a lot more than the measurements from the experiment with the monopile model showed. One factor that was expected to be of importance, are the viscous effects. Viscous effects could play a role during piston mode in a monopile by increasing damping at the sharp edges of the structure, resulting from vortex shedding or energy dissipation at the edges, which could limit the extent of water motion within the monopile. However, one would expect viscous damping to be of highest influence when the piston mode resonance is induced, while in the results, where vertical lines are drawn in the figure to point out piston mode resonance and sloshing, the piston mode amplitudes for the monopile were approaching the moonpool amplitudes when the resonance mode was induced. This indicates that something else is going on that is of larger influence than the viscous effects, when comparing a monopile to a moonpool during piston mode resonance. The explanation of this phenomena remains inconclusive from the results of this research.

The plot of draft 1 (=0.34) looks different than the plots for the larger drafts. The experiments with draft 1 also visibly showed more and different resonance effects. At wave length 2.59m piston mode resonance was visible but also sloshing was observed, even side-way sloshing. At wave length 3.33m, both sloshing and piston modes were visible as well as side way sloshing. For the higher waves, not much response in the inner water column was visible except that water level just moving at the same height as the waves that were passing the cylinder. Since these waves were much longer than the cylinder's diameter, the whole water surface in and around the cylinder went up and down during a wave.

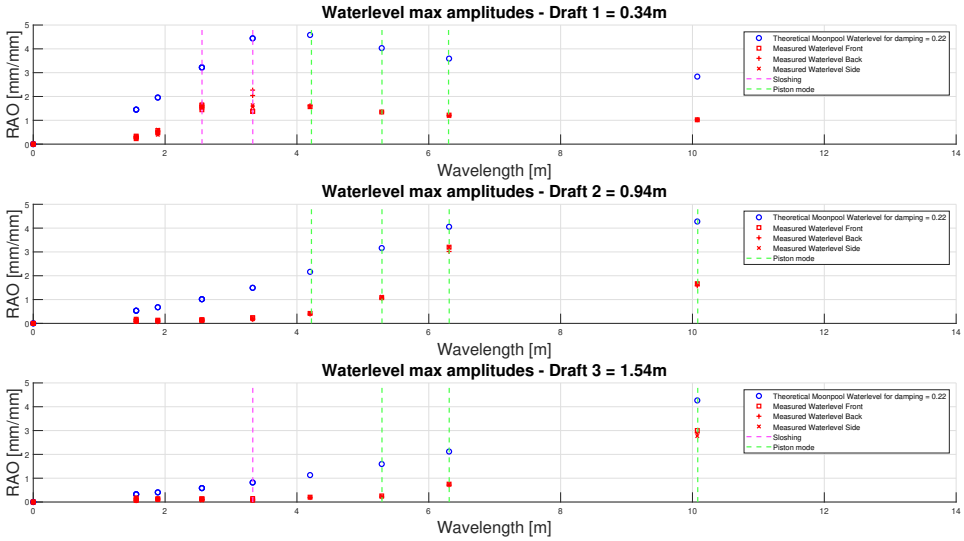

Figure 4.18: Water Level amplitudes normalized by wave amplitudes, damping ratio = 2.2%

For the deeper drafts, draft 2 (=0.94m) and draft 3 (=1.54m) The shorter waves theoretical water level amplitudes exceed the measured data. The theoretical values are calculated using theory for moonpools [12] [17]. Their geometry is fundamentally different from monopiles, because moonpools are surrounded by a ship and monopiles have thin walls. The theory for moonpools might overestimate the monopile measurements because of viscous effects at sharp edges.

At draft 2, from the wavelength of 5.29m onward, the theoretical and measured value both have an increased amplitude. In moonpool theory, piston mode resonance is expected at this wavelength, causing the amplitude to rise. In the monopile experiment, piston mode resonance was observed for this wavelength, but the amplitude of the piston mode is not as high as would be expected for the moonpool. The same pattern is visible for wavelengths 6.29m and 10.1m. During the experiments for draft 2, piston mode resonance was visible for those three longest waves. No resonant behavior was observed in the other waves.

At draft 3, we see that from the wavelength of 6.29m the theoretical and measured data seem to have similar values. However, at a wavelength of 10.1m the theoretical amplitude is 6 times higher than the measured amplitude. Moonpool theory expects large amplitudes at this wavelength, but the measured values for the monopile do not get as large. During the experiment for draft 3, piston mode was observed in the three longest waves and sloshing was observed for wavelengths 3.33m. No resonant behavior was observed in other waves.

The results indicate that the hydrodynamic behavior of the inner water column in a monopile differs from theoretical predictions based on moonpool resonance theory, primarily due to differences in geometry and water displacement effects. While moonpool theory can be useful for determining the piston mode resonance frequencies, the lower water level amplitudes observed in the monopile suggest that monopile designs may experience reduced wave-induced motions compared to moonpools. For offshore operations, this implies that internal resonance effects may be less critical for monopile installations than anticipated using moonpool theory, potentially simplifying operational planning.

4.4. Relation Between Inner Water Column Behavior and Hydrodynamic Forces

Looking back at figures 4.5, 4.6 and 4.7 of the force amplitudes and figures 4.9, 4.8 and 4.10 of the moment amplitudes, the following conclusions can be drawn on the influence of inner water column behavior on hydrodynamic forces and moments.

The resonance responses during the experiment are displayed in table 4.1.

Wave length	Draft 1 (=0.34m)	Draft 2 (=0.94m)	Draft 3 (=1.54m)
1.56m	-	-	-
1.89m	-	-	-
2.56m	side-way sloshing	-	-
3.33m	side-way sloshing	-	sloshing
4.20m	piston mode	piston mode	-
5.29m	piston mode	piston mode	piston mode
6.29m	piston mode	piston mode	piston mode
10.1m	-	piston mode	piston mode

Table 4.1: Visually observed Resonance Modes During Experiment

Regarding the Fx amplitudes, the measurement does not suggest the forces to be higher when resonance modes are induced, compared when they are not induced. For the Fy amplitudes, the forces measured during resonance are not specifically higher than the forces measured when there was no resonant behavior.

Overall, the influence of resonance modes on hydrodynamic forces and moments is not large. Resonance adds energy to the inner water column, but this does not consistently show up as larger forces or moments in the measurements. One possible explanation is that much of the energy from the inner water column is damped at the sharp edges of the monopile, so only part of it affects the overall dynamics. On top of that, the low Keulegan-Carpenter (KC) numbers in this study suggest that inertial forces dominate, which may limit the role of resonance effects in these specific experiments. At low KC numbers, the water mostly moves around the monopile without much swirling or flow separation. This makes the forces be influenced mostly by the mass and acceleration of the water. Because inertia is the dominant force, the extra motion caused by resonance doesn't have as much influence.

These results show that while there is some connection between wave-induced resonance and hydrodynamic forces, it is not very strong. For these conditions, resonance does not lead to big increases in forces or moments, but it is still worth paying attention to. Resonance modes in monopiles might become more important in other situations or at different scales.

4.5. Additional Observations

Some variations are observed at specific wavelengths, such as around 2 m in Draft 1, where sloshing and sideways sloshing were noted during the experiment. Ideally, sideways sloshing should not occur in a perfectly symmetric setup with a vertical cylinder. However, minor imperfections in the experimental conditions could have triggered these behaviors. For instance, the cylinder might not be perfectly round or perfectly vertical, introducing a small offset.

In circular confinements, even a slight deviation can initiate sloshing due to asymmetries in wave impact or flow behavior. Once sloshing begins, it requires only a minimal imbalance to develop into sideways sloshing, where the inner water oscillates in a swirling motion. Research indicates that sloshing modes in circular or open-bottom structures are sensitive to initial conditions. When the water begins oscillating laterally or swirling, even small imbalances can sustain or amplify these motions, as the symmetry of the enclosure does not inherently dampen them. This behavior has been observed in experiments and numerical studies on resonance in circular geometries, where small perturbations could result in significant lateral or swirling motions, particularly near the natural sloshing frequencies [32]. Figures 4.19 and 4.20 show observed lateral sloshing and swirling motions in the experiment.

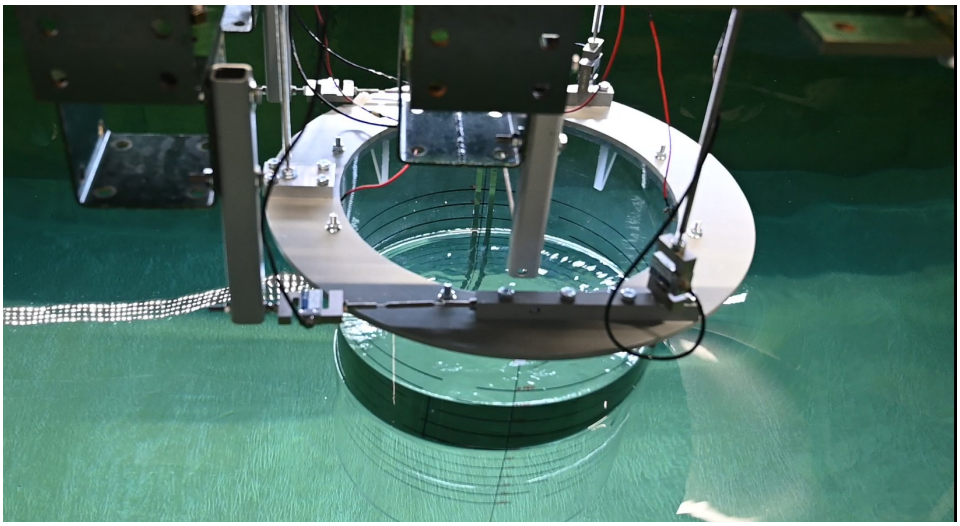

Figure 4.19: Side-Ways/Lateral Sloshing

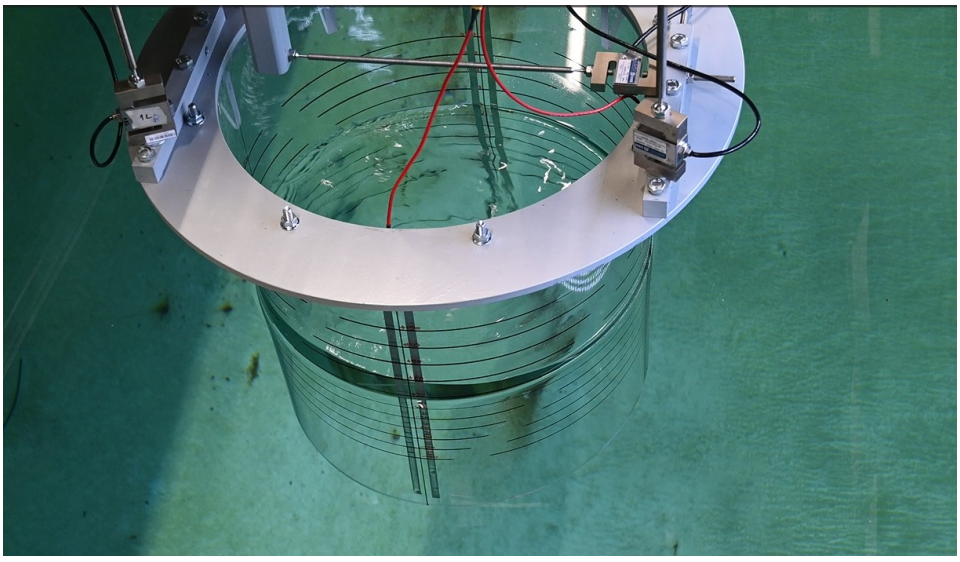

Figure 4.20: Swirling Sloshing

Sloshing inside the monopile has direct implications for offshore installation procedures. During lowering operations, sloshing motions can increase the forces acting on the monopile structure. This is particularly critical at specific drafts where resonance is likely to occur. For example, strong sloshing or swirling can amplify lateral forces, causing unexpected tilting or misalignment.

Understanding sloshing behavior also helps define safe conditions for lowering, where resonance effects are minimized. By identifying the conditions that cause sloshing or sideways sloshing, operational strategies can be developed to avoid these critical scenarios.

4.6. Summary

The results from the wave tank experiments provide important insights into the hydrodynamic behavior of large-diameter monopiles during a vertical lowering operation. Several observations have implications for both theoretical models and practical offshore installation procedures.

Using Solid Cylinder Theory on Monopile is useful because solid cylinder theory using Morison works quite well, especially for larger wavelengths. However, shorter wave lengths are most present in the north sea and as monopile diameters increase, the wavelength that is considered ”short” will get larger since Morison is applicable for wavelengths that are at least 6 times larger than the monopiles diameter. This means Morison method gets less applicable when monopile diameters increase.

Using Moonpool Theory on Monopile is useful because moonpool theory works well for predicting sloshing and piston mode resonance frequencies for a vertical monopile. Moonpool theory overestimates the height of the piston mode, meaning it is a conservative method to use for calculations on monopiles. However, for the calculation of hydrodynamic forces on a large diameter monopile during a lowering operation, the results of this study show that the height of the piston mode is not a concern, as moonpool theory is conservative and the hydrodynamic forces are not largely influenced by the piston resonance mode.

Sloshing and Sideways Sloshing occurred in the experiments at specific wavelengths, particularly around 2 m at Draft 1. This behavior is sensitive to initial conditions, as even small imperfections in the experimental setup—such as slight asymmetries in the cylinder or its positioning—can initiate sloshing. Once sloshing begins, it can lead to sideways sloshing, where the water oscillates in a swirling motion. This phenomenon is crucial for offshore operations, as sloshing can significantly amplify the forces acting on the monopile, leading to potential misalignment or tilting during the lowering process. The lateral forces, generated by sloshing, particularly in shallow drafts, can impact the stability of the monopile during installation.

Operational Implications are that during the lowering operation, resonance effects especially from sloshing at shallow drafts, can lead to increased hydrodynamic force on the monopile, causing unexpected tilting or misalignment. Understanding the resonance behavior and sloshing dynamics is useful for optimizing monopile installation procedures. Identifying and avoiding the draft and wave conditions that lead to resonance will be advised for minimizing operational risks. By developing operational strategies that take these resonance conditions into account, the safety and efficiency of offshore monopile installations can be improved.

5

Conclusion and Recommendations

This thesis investigated the hydrodynamic forces acting on a large diameter monopile during a vertical lowering operation. By examining the monopile's response under various wave conditions and drafts experimentally, the study provides valuable insights into the unique hydrodynamic characteristics of the structure, bridging the gap between existing theories for solid cylinders and moonpools.

5.1. Findings

The study confirmed that inertial forces dominate under the low Keulegan-Carpenter (KC) number conditions in the North Sea (maximum $KC = 0.76$). The relevance of specific wave and current conditions was validated through realistic offshore scenarios, emphasizing the importance of wave height and wave length in influencing the monopile's behavior. The forces and moments on the monopile at wavelengths longer than 6 times the diameter were generally well-described by the Morison equation, using inertia coefficient $C_m = 1.5$ and drag coefficient $C_d = 1.0$. This means that using the Morison equation, which is originally designed for solid cylinders, to account for the hollow, surface-piercing structure of the monopile, is possible. From this the conclusion can be drawn that the column of water inside the vertical monopile in these conditions, provides a similar inertia as if the cylinder had been solid. For waves with wave lengths shorter than 6 times the monopile's diameter, the Morison equation is conservative at it predicts the forces and moments larger than actually measured. The shorter the wave, the larger the force is overestimated. The shortest wave in this research with a wave length of 1.88 meters was overestimated using Morison by approximately 400% of the actual measured force. This means as monopile diameters increase, the Morison equation will be less applicable for the prediction of forces and moments in a realistic offshore scenario for the North Sea. This means other methods, like computational fluid dynamics, have to be used to be able to get a good estimate of wave forces and moments on a large-diameter monopile.

The significant difference between solid cylinders and monopiles is the presence of the inner water column. This column showed resonance phenomena such as sloshing and piston mode. Theoretical predictions based on moonpool resonance frequencies were consistent with observed resonance frequencies in the vertical monopile, although for prediction the amplitudes of the water motion during resonant behavior the moonpool theory is conservative as it overestimates these amplitudes by 30% up to 300%.

As for the effects of the resonance phenomena on the hydrodynamic forces and moments, the conclusion can be drawn that the impact of these modes on the hydrodynamic forces was limited. Based on the measured data, forces in x-direction and moments around the y-axis are not influenced by resonance modes. During piston mode, sloshing (in x-direction) and sideway sloshing (sloshing in y-direction) the forces in y-direction and z-direction increased by 25% to 50% compared to when this resonance mode was not induced, however still having small amplitudes of 3 N/mm (at draft = 0.34m) to 6 N/mm (at draft = 1.54m). In experimental conditions with monochromatic waves induced from one direction, high forces in the orthogonal direction to the waves are not expected. However, in an offshore environment like the North Sea, multi-directional waves and currents are expected and therefore the monopile is supported in all directions. This means it is not expected that these small

increase in forces in orthogonal direction due to piston mode and sloshing will be of influence in an offshore vertical installation of a large-diameter monopile.

Draft variations played a role in influencing monopile resonance behavior. Shallow drafts showed resonance effects for shorter waves, while deeper drafts were less influenced for shorter waves. These findings show the importance of draft-specific considerations in vertical monopile installation procedures.

The results of this study indicate that viscous effects, while potentially contributing to increased damping and reducing piston mode amplitudes, do not significantly affect the hydrodynamic forces or alter the resonance frequencies of the monopile. The piston mode amplitudes are substantially lower than those predicted by moonpool theory, sometimes by as much as 300%, and the resonance modes do not introduce large additional hydrodynamic forces. Therefore, in large-scale vertical monopile lowering operations, viscous effects can be considered negligible.

5.2. Implications for Offshore Installation

The findings show the need for accurate modeling of hydrodynamic forces during a vertical monopile installation to ensure operational safety and efficiency. The Morison equation, with coefficient modifications, provides a good force estimation in many scenarios. However, its limitations for shorter waves show a need for other approaches when monopiles grow in size.

Resonance phenomena, while visually significant, were shown to have a minimal effect on force magnitudes. Nevertheless, their influence on local dynamics and potential implications for structural stability should not be overlooked. During installation operations, draft-specific effects should be accounted for to minimize operational risks.

5.3. Model Limitations and Future Research

This study prioritized inertial forces due to the dominance of these effects under the tested conditions. Viscous effects, particularly around the monopile's sharp edges and free end, were acknowledged but not extensively explored. Future research should investigate these effects in more detail, especially in extreme conditions where viscous forces might play a more significant role.

Expanding the range of wave conditions studied, including more extreme sea states, could validate the findings of this study. Additionally, exploring three-dimensional wave and current effects and combining these with practical installation scenarios, like a lifting arrangement or for scenarios where the monopile is not vertically submerged in the water but tilted, could provide deeper insights into monopile behavior under realistic offshore conditions.

5.4. Concluding Remarks

By using theories for solid cylinders and moonpools, the study provides a foundation for improving predictive models and installation practices. The emphasis on inertial dominance, draft-specific effects, and resonance phenomena helps the understanding of hydrodynamic forces on a large-diameter monopile during a vertical lowering operation and offers valuable guidance for the safe and efficient installation of monopiles in offshore environments.

Bibliography

[1] E. Engineering, *The Empire Engineering Guide to Offshore Wind Foundations - 2nd Edition*. 2023. [Online]. Available: https://www.empireengineering.co.uk/guide-to-offshore-wind-foundations/.

[2] M. Dam, "Monopile installation assessment," Master Thesis, TU Delft, Delft, Jun. 2018. [Online]. Available: https://repository.tudelft.nl/islandora/object/uuid%3A719004c8-832c-4564-a6e6-38b3f365937b.

[3] J. Journée and W. Massie, *Offshore Hydromechanics*. Delft: Delft University of Technology, Jan. 2001.

[4] M. O. J.R. Morison, "The force exerted by surface waves on piles," *Petrol Trans AIME*, 1950.

[5] M. Benitz, D. Carlson, B. Seyed-Aghazadeh, Y. Modarres-Sadeghi, M. Lackner, and D. Schmidt, "Cfd simulations and experimental measurements of flow past free-surface piercing, finite length cylinders with varying aspect ratios," en, *Computers and Fluids*, vol. 136, pp. 247–259, Sep. 2016, ISSN: 00457930. DOI: 10.1016/j.compfluid.2016.06.013.

[6] D. Hamel-Derouich, "Hydrodynamic forces on rectangular cylinders of various aspect ratios immersed in different flows," PhD Thesis, University of Glasgow, Glasgow, 2020. [Online]. Available: https://theses.gla.ac.uk/74858/.

[7] A. Boon, "Drag of a surface piercing cylinder in fast current and low waves," Master Thesis, TU Delft, Delft, 2020. [Online]. Available: https://repository.tudelft.nl/record/uuid:ac9c9975-88df-404e-9a61-33438abc0b5f.

[8] G. Yu, E. J. Avital, and J. J. R. Williams, "Large eddy simulation of flow past free surface piercing circular cylinders," en, *Journal of Fluids Engineering*, vol. 130, no. 10, p. 101 304, Oct. 2008, ISSN: 0098-2202, 1528-901X. DOI: 10.1115/1.2969462.

[9] B. Koo, J. Yang, S. M. Yeon, and F. Stern, "Reynolds and froude number effect on the flow past an interface-piercing circular cylinder," en, *International Journal of Naval Architecture and Ocean Engineering*, vol. 6, no. 3, pp. 529–561, Sep. 2014, ISSN: 20926782. DOI: 10.2478/IJNAOE-2013-0197.

[10] M. Mohseni, P. T. Esperanca, and S. H. Sphaier, "Numerical study of wave run-up on a fixed and vertical surface-piercing cylinder subjected to regular, non-breaking waves using openfoam," en, *Applied Ocean Research*, vol. 79, pp. 228–252, Oct. 2018, ISSN: 01411187. DOI: 10.1016/j.apor.2018.08.003.

[11] S. Chen, W. Zhao, and D. Wan, "Turbulent structures and characteristics of flows past a vertical surface-piercing finite circular cylinder," en, *Physics of Fluids*, vol. 34, no. 1, p. 015 115, Jan. 2022, ISSN: 1070-6631, 1089-7666. DOI: 10.1063/5.0078526.

[12] B. Molin, "On the piston and sloshing modes in moonpools," *Journal of Fluid Mechanics*, vol. 430, pp. 27–50, Mar. 2001, ISSN: 00221120. DOI: 10.1017/S0022112000002871.

[13] L. Lu, L. Cheng, B. Teng, and M. Zhao, "Numerical investigation of fluid resonance in two narrow gaps of three identical rectangular structures," en, *Applied Ocean Research*, vol. 32, no. 2, pp. 177–190, Apr. 2010, ISSN: 01411187. DOI: 10.1016/j.apor.2009.10.003.

[14] O. M. Faltinsen, O. F. Rognebakke, and A. N. Timokha, "Two-dimensional resonant piston-like sloshing in a moonpool," en, *Journal of Fluid Mechanics*, vol. 575, pp. 359–397, Mar. 2007, ISSN: 0022-1120, 1469-7645. DOI: 10.1017/S002211200600440X.

[15] T. Kristiansen, "Two-dimensional numerical and experimental studies of piston-mode resonance," Doctoral thesis, NTNU, Trondheim, Apr. 2009. [Online]. Available: https://ntnuopen.ntnu.no/ntnu-xmlui/bitstream/handle/11250/237666/218240_FULLTEXT01.pdf?sequence=1.

[16] S. Ravinthrakumar, T. Kristiansen, B. Molin, and B. Ommani, “A two-dimensional numerical and experimental study of piston and sloshing resonance in moonpools with recess,” en, vol. 877, pp. 142–166, Oct. 2019, ISSN: 0022-1120, 1469-7645. DOI: 10.1017/jfm.2019.561.

[17] T. Kristiansen and O. M. Faltinsen, “Gap resonance analyzed by a new domain-decomposition method combining potential and viscous flow,” en, *Applied Ocean Research*, vol. 34, pp. 198–208, Jan. 2012, ISSN: 01411187. DOI: 10.1016/j.apor.2011.07.001.

[18] A. G. Fredriksen, T. Kristiansen, and O. M. Faltinsen, “Wave-induced response of a floating two-dimensional body with a moonpool,” en, *Philosophical Transactions of the Royal Society A: Mathematical, Physical and Engineering Sciences*, vol. 373, no. 2033, p. 20 140 109, Jan. 2015, ISSN: 1364-503X, 1471-2962. DOI: 10.1098/rsta.2014.0109.

[19] S. Ravinthrakumar, T. Kristiansen, B. Molin, and B. Ommani, “Coupled vessel and moonpool responses in regular and irregular waves,” en, *Applied Ocean Research*, vol. 96, p. 102 010, Mar. 2020, ISSN: 01411187. DOI: 10.1016/j.apor.2019.102010.

[20] J. Han, X. Zhang, and H. Huang, “Experimental and numerical studies of piston-mode resonance in a three-dimensional circular moonpool,” en, *Physics of Fluids*, vol. 35, no. 8, p. 082 106, Aug. 2023, ISSN: 1070-6631, 1089-7666. DOI: 10.1063/5.0160461.

[21] B. Veritas, *Guidance note ni 621 dt r01 e - hydrodynamic analysis of offshore floating structures*, Accessed: 2023-12-23, 2016. [Online]. Available: https://erules.veristar.com/dy/data/bv/pdf/621-NI_2016-01.pdf.

[22] S.-Y. Han, B. Bouscasse, V. Leroy, *et al.*, “Experimental study of wave diffraction loads on a vertical circular cylinder with heave plates at deep and shallow drafts,” *Ocean Engineering*, vol. 284, p. 118 970, 2024, Accessed: 2024-12-24. DOI: 10.1016/j.oceaneng.2024.118970. [Online]. Available: https://doi.org/10.1016/j.oceaneng.2024.118970.

[23] R. W. Clough and J. Penzien, *Dynamics of Structures*, 2nd. New York: McGraw-Hill, 1993, ISBN: 9780071132411.

[24] S. Lindemann, *Consulting: XXL monopile*. [Online]. Available: https://seawind.eu/expertise/xxl-monopile/.

[25] Q. S. G. of the 28th ITTC, *Ittc quality system manual - recommended procedures and guidelines: Guideline for viv testing*, 2014. [Online]. Available: https://www.ittc.info/media/8131/75-02-07-0310.pdf.

[26] LibreTexts Team, *Capillary action*, Accessed: 2024-12-12, n.d. [Online]. Available: https://chem.libretexts.org/Bookshelves/Physical_and_Theoretical_Chemistry_Textbook_Maps/Supplemental_Modules_(Physical_and_Theoretical_Chemistry)/Physical_Properties_of_Matter/States_of_Matter/Properties_of_Liquids/Capillary_Action.

[27] C. Tsai and T. Yen, “Fabrication of super-hydrophobic film from pmma with intrinsic water contact angle below 90°,” *Journal of Membrane Science*, vol. 317, pp. 256–264, 1-2 2008, Accessed: 2024-12-12. DOI: 10.1016/j.memsci.2008.02.038. [Online]. Available: https://www.researchgate.net/publication/222079685_Fabrication_of_super-hydrophobic_film_from_PMMA_with_intrinsic_water_contact_angle_below_90.

[28] MathWorks. “Amplitude estimation and zero-padding.” Accessed: 2024-12-09. (2024), [Online]. Available: https://nl.mathworks.com/help/signal/ug/amplitude-estimation-and-zero-padding.html.

[29] P. Gujer, “Overall damping for piled offshore support structures,” *GL RC Guideline for the Certification of Offshore Wind Turbines, Edition 2005*, 2005.

[30] S. Gres, M. Fejerskov, L. B. Ibsen, and L. Damkilde, “Experimental damping assessment of a full scale offshore mono bucket foundation,” *Proceedings of ISMA2016: International conference proceedings on noise and vibration engineering (pp. 4045-4054)*, 2016.

[31] T. Kristiansen and O. Faltinsen, “Application of a vortex tracking method to the piston-like behaviour in a semi-entrained vertical gap,” *Applied Ocean Research*, vol. 30, no. 1, pp. 1–16, 2008, ISSN: 0141-1187. DOI: https://doi.org/10.1016/j.apor.2008.02.003. [Online]. Available: https://www.sciencedirect.com/science/article/pii/S0141118708000102.

[32] S. Ravinthrakumar, “Wave-induced resonant flow in moonpools with and without recess,” Accessed November 21, 2024, Ph.D. dissertation, Norwegian University of Science and Technology (NTNU), 2023. [Online]. Available: https://ntnuopen.ntnu.no/ntnu-xmlui/handle/11250/3129312.